الجمهورية الجزائرية الديمقراطية الشعبية
République algérienne démocratique et populaire
وزارة التعليم العالي والبحث العلمي
Ministère de l'enseignement supérieur et de la recherche scientifique
جامعة عين تموشنت بلحاج بوشعيب
Université –Ain Temouchent- Belhadj Bouchaib
Faculté des Sciences et de Technologie
Département de Génie Mécanique

Projet de Fin d'Etudes
Pour l'obtention du diplôme de Master en : Construction Mécanique
Domaine : Science et Technologie
Filière : Génie Mécanique
Spécialité : Construction Mécanique

Thème

NUMERICAL STUDY OF ELLIPTICAL CRACKS IN PIPELINE WITH A THICKNESS TRANSITION UNDER TRACTION COMPRESSION LOADING

Présenté Par :
1) M. SIWELA Mbongeni
2) M. DANOMAH Thomas

Devant le jury composé de :

Dr. BELHAMIANI M.		UAT.B.B (Ain Temouchent)	Président
Dr. BAHRAM K.		UAT.B.B (Ain Temouchent)	Examinateur
Pr. OUDAD W.	M C A	UAT.B.B (Ain Temouchent)	Encadrant

Année Universitaire 2022/2023

ACKNOWLEDGEMENTS

First and foremost, we express our gratitude to the Almighty God for his mercy and the gift of life, as well as for giving us the bravery, determination, and perseverance to do this task.

We owe a lot to our supervisor, Mr. Oudad Wahid, a professor at the University of Ain Temouchent, whose presence, support, and open-mindedness are hidden behind this work. We are especially grateful to him for accepting to direct this project and for his insightful counsel as it was being developed.

We would also like to convey our sincere gratitude to the president of the jury, Dr. Belhamiani M., the examiner, Dr. Bahram K. for agreeing to honor us by evaluating our work.

Additionally, the stuff members of the department and the faculty of science and technology at the University of Ain Témouchent, as well as the teachers in the field of industrial engineering, are all greatly appreciated.

Last but not least, we would like to express our gratitude to all of our families for their unwavering support as well as to everyone else who helped bring this project to fruition through their direct and indirect contributions.

DEDICATION

We dedicate this project to the Almighty God our creator, our strong pillar, and our source of inspiration, wisdom, knowledge and understanding. He has been the source of our strength throughout this academic journey and on His wings only have we soared.

We also dedicate this project to our families. They instilled in us the desire to learn and made sacrifices so that we would have access to high quality education from an early age. Also, this is dedicated to our teachers and colleagues who have always supported us throughout our year of studies.

ABSTRACT

Pipelines used to transfer gas and oil are typically buried in the ground and are internally and externally coated with steel that has strong mechanical qualities. However, it turns out that these pipes are susceptible to damage brought on by a lack of substance or cracks. Therefore, rigorous study must be done throughout the service life of these pipelines in order to predict and prevent catastrophic failures of these structures. Thus, the subject of our investigation will be semi-elliptical cracks in pipes with a thickness transition. This structure consists of two butt-welded pipes of thickness t_1 and t_D. The thickness of the pipes varies linearly inside the transition zone. The influence of the crack's shape, the crack's position, and the type of loading on the stress intensity factor (SIF) in mode I is examined using a numerical simulation based on the three-dimensional finite element method (FEM) utilizing the ABAQUS 6.14 computer code.
Keywords: Thickness transition, semi-elliptical cracks, stress intensity factor (SIF)

RESUME

Les pipelines utilisés pour le transfert de gaz et de pétrole sont généralement enfouis dans le sol et revêtus intérieurement et extérieurement d'acier aux qualités mécaniques importantes. Cependant, il s'avère que ces conduites sont susceptibles d'être endommagées par un manque de substance ou des fissures. C'est pourquoi une étude rigoureuse doit être menée tout au long de la durée de vie de ces canalisations afin de prévoir et de prévenir les défaillances catastrophiques de ces structures. Ainsi, le sujet de notre étude sera centré sur les fissures semi-elliptiques dans les conduites avec une transition d'épaisseur. Cette structure se compose de deux tuyaux soudés bout à bout d'épaisseur t_1 et t_D. L'épaisseur des tubes varie linéairement à l'intérieur de la zone de transition. L'influence de la forme des fissures, de leur position, et du type de chargement sur le facteur d'intensité des contraintes (FIC) en mode I est examinée à l'aide d'une simulation numérique basée sur la méthode des éléments finis (FEM) tridimensionnelle utilisant le code informatique ABAQUS 6.14.
Mots-clés : Transition d'épaisseur, fissures semi-elliptique, facteur d'intensité des contraintes (FIC).

List of abbreviations

EDF:	Electricité de France
LEFM:	Linear-Elastic Fracture Mechanics
EPFM:	Elastic-Plastic Fracture Mechanics
SIF:	Stress Intensity Factor
CTOD:	Crack Tip Opening Displacement
ASME:	American Society of Mechanical Engineers
BPVC :	Boiler and Pressure Vessel Code
HSE:	Health and Safety Executive
SMAW:	Shielded Metal Arc Welding
SAW:	Submerged Arc Welding
GMAW:	Gas-Metal Arc Welding
GTAW:	Gas-Tungsten Arc Welding
ERW:	Electric Resistance Welding
SMLS:	Seamless Pipe
SSAW:	Spiral Submerged Arc Welding
MIC:	Microbiologically Induced Corrosion
SCC:	Stress Corrosion Cracking
EAC:	Environmental Assisted Cracking
HIC:	Hydrogen Induced Cracking
PI:	Pipeline Integrity
PIM:	Pipeline Integrity Management
MFL:	Magnetic Flux Leakage
TFI:	Transverse Field Inspection
UT:	Ultrasonic
GPS:	Global Positioning System
API:	American Petroleum Institute
CAE:	Complete Abaqus Environment
CLs:	Condition Limit

LIST OF FIGURES

CHAPTER 1:

CHAPTER 2:

CHAPTER 3

LIST OF TABLES

List of nomenclatures

σ_{max} :	maximum stress at the end of the major axis [MPa]
σ_a:	applied stress applied normal to the major axis [MPa]
a:	crack depth [mm]
c:	half major axis or half crack length [mm]
ρ:	radius of curvature [mm]
k_t :	stress concentration factor
k_c:	fracture toughness [MPa.mm$^{0.5}$]
G:	energy release rate [J/m^2]
K:	stress intensity factor [MPa.mm$^{0.5}$]
E:	Young's modulus [GPa]
G_c:	critical energy release rate [J/m^2]
γ_s:	the surface energy [J/m^2]
γ_p:	energy of plastic deformation [J/m^2]
r_y:	plastic zone [mm]
σ_{ys}:	yield strength [MPa]
W:	strain energy density [J/m^3]
T:	components of the traction vector
∂u:	displacement vector components
ds:	length increment along the contour Γ [mm]
Γ:	arbitrary contour around the crack tip
σ_{ij}:	stress tensors
ε_{ij}:	strain tensors
n_j:	components of the unit vector normal to Γ

Contents

GENERAL INTRODUCTION

GENERAL INTRODUCTION

Pipelines have long been the most affordable and secure way to move fluids in huge amounts and over long distances, especially gas and oil. However, they are frequently subjected to damage threats that could impair their function or potentially have a negative impact on the environment and the safety of the general public. This emphasizes how important the integrity of these structures is. Historically, many accidents occurred as a result of the neglect of fracture mechanics. Among the most famous accidents, we cite the sinking of the vessel 'Liberty Ship' in the port of New York caused by the effect of stress concentration and cold [1].

Fracture mechanics has thus been an essential tool in industrial structures, pressure vessels and more generally metal structure's design. It is typically used to forecast component failure brought on by minor cracks within the structure. It thus enables us to take preventive measures to stop the fracture from spreading further or, in the event that spreading is inevitable, to estimate the lifespan of the structure. The foundation of fracture mechanics is a mathematical description of the stress region surrounding a crack in a loaded body.

For the integrity assessment of structures with fractures, the stress intensity factor (SIF) K suggested by Irwin [2] serves as the primary fracture parameter. Other crack propagation methods have been studied with varying degrees of success for elastoplastic and viscoplastic behavior.

The failure behavior of cracks can be assessed by the stress intensity factor (SIF) K or the J integral [1], [2] on a global scale as often performed by finite element (FE) calculations [3].

To ensure high safety, a substitution geometry must be more vulnerable to failure. For complex geometries, it is generally desired to simplify the problem to simpler geometries whose calculations are less expensive [4], [5], [6] which is not the case for thickness transitions. A study conducted by the French company EDF and the CEA on cylinders with a thickness transition [6]. In this study [6], it was shown that the use of SIF as a critical parameter for elastic materials of a cylinder of uniform thickness for the calculations of K_I in the thickness transition gave conservative results and accurate.

In our study, we use the finite element method to investigate how an elliptical crack in a pipeline with a thickness transition responds to pressure and stress loading. The examination of the many changes of the stress intensity factor in mode 1 (K_I) with various crack geometries, crack positions and loading types is the main emphasis of the work. We also consider how this K_1

may change if a scratch were to be introduced to various positions along a fractured pipe with a thickness transition. Lastly, a comparison of the effect of a crack in a pipe with a thickness transition, a pipe with uniform thickness, and a scratched pipe with a thickness transition is made.

This document is split into three sections:

Chapter 1 presents an overview of the major fracture mechanics theories that have been used on metal structures and pressure pipes. We specifically provide an introduction to elastoplastic and linear elastic fracture mechanics.

The goal of Chapter 2 is to provide a general overview of pipelines. We present the definition of a pipeline and its constituent parts, the various kinds of pipelines that exist and how they are made, the damages they sustain, and lastly the integrated pipeline system.

Chapter 3 covers the elastic modeling of the simulation-treated structure (finite elements) and the data gathering from the pipe under study. We then present the findings and discuss them before drawing a broad conclusion.

CHAPTER 1

FRACTURE MECHANICS

CHAPTER 1

FRACTURE MECHANICS

1.1 Introduction

Fracture mechanics is based on the implicit assumption that there is a crack in a work component. The crack may be man-made, such as a hole, a notch, a slot, a re-entrant corner, etc. The crack may exist within a component due to manufacturing defects like slag inclusion, cracks in a weldment, or heat affected zones due to uneven cooling and the presence of foreign particles. A dangerous crack may be nucleated and grow during the service of the component (fatigue generated cracks, nucleation of notches due to environmental dissolution) [3].

Fracture mechanics is also applied to crack growth under fatigue loading. Initially, the fluctuating load nucleates a crack, which then grows slowly, and finally the crack growth rate per cycle picks up speed (see Figure 1-1) [7]. Thereafter comes the stage when the crack-length is long enough to be considered critical for a catastrophic fracture failure. A mathematical analysis of the stress distribution that surrounds a crack in a loaded structure serves as the basis for fracture mechanics, that explain how solids or structures behave when there is a geometrical discontinuity in the size of the structure.

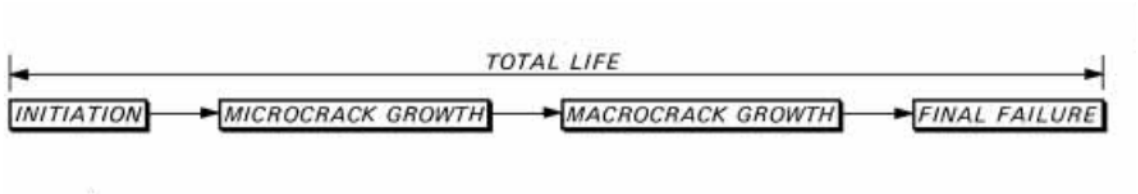

Figure 1- 1 Schematic representation of fatigue life [8].

1.2 Important variables in fracture mechanic's approach

i. Applied stress

ii. The flaw size in the structure

iii. Fracture toughness

1.3 Types of fracture

In order to clearly progress in fracture mechanics, the main fracture mechanisms of the metals must be well studied and understood. *Fracture is the separation of a solid body into two or*

more pieces under the action of stress [1]. The tensile test of metal components can be an indicator for the observation of the fracture types. Hence, according to the strain to fracture behavior of materials, there are two types of fractures, namely:

a. Brittle fracture

Brittle fracture or failure takes place with little or no preceding plastic deformation. It occurs often at unpredictable levels of stress through rapid crack propagation. The direction of crack propagation is very nearly perpendicular to the direction of applied tensile stress [9]. It is often possible to reassemble brittlely fragmented pieces of materials or components without appreciably changing their original shape or size (see Figure 1-2).

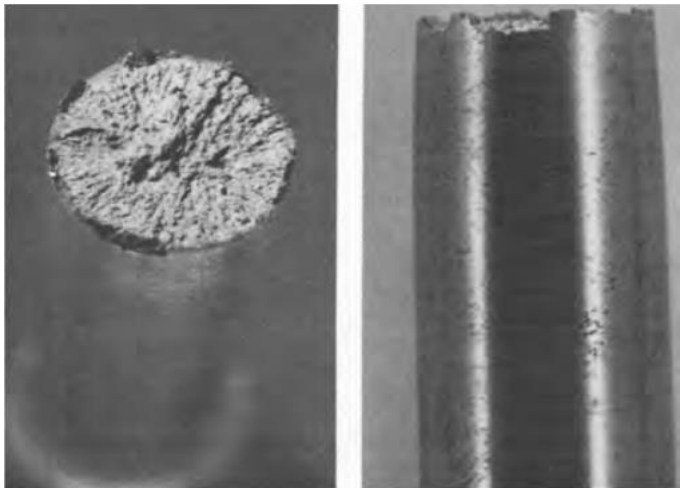

Figure 1- 2 Brittle fracture [1].

There are two major types of brittle fractures, namely:

i. Transgranular brittle fracture (cleavage)

A brittle fracture is caused by cleavage. Cleavage generally takes place through the separation of atomic bonds along well-defined crystal planes. Cleavage propagating through one grain changes direction as it crosses a grain or subgrain boundary (subgrains are regions within a grain that differ slightly in crystal orientation), as shown in Figure 1-3 [8].

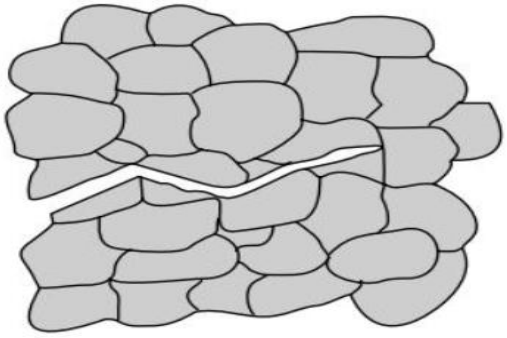

Figure 1- 3 Transgranular brittle fracture [3].

ii. Intergranular brittle fracture

This type of fracture involves the spreading of cracks along a metal's or alloy's grain boundaries. Instead of passing through the actual grains, intergranular fractures move along the grain borders.

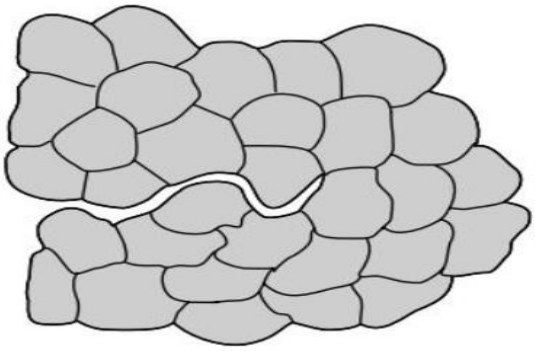

Figure 1- 4 Intergranular brittle fracture [3].

b. Ductile fracture

Ductile fracture is a mode of material failure in which voids, either already existing within the material, or nucleated during deformation, grow until they link together, or coalesce, to form a continuous fracture path. Other terms used for this fracture mode are fibrous fracture, dimpled rupture, or microvoid coalescence. The material deforms plastically, and this plastic deformation and coalescence of voids absorb a large amount of energy therefore, a crack does not grow easily in ductile materials [10], [4].

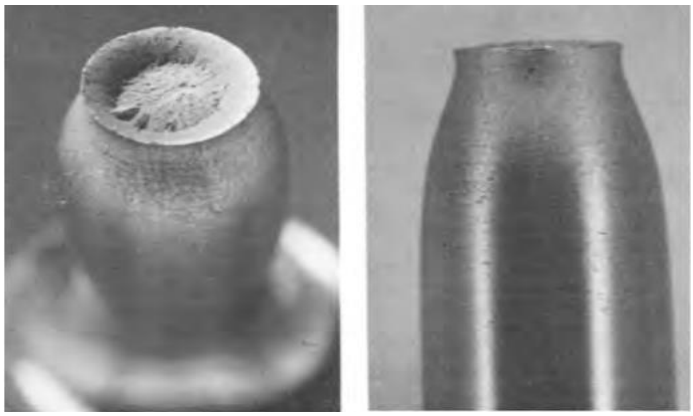

Figure 1- 5 Ductile fracture [1].

1.4 Fracture toughness k_c

Fracture toughness k_c generally termed as a resistance of a material to the propagation of a crack. Fracture toughness is an indication of the amount of stress required to propagate the pre-existing crack. So, fracture toughness testing and evaluation has been a very important subject in development of fracture mechanics method and its engineering applications [5].

The fracture toughness values are also used as a basic in following:

i. Material characterization
ii. Performance evaluation
iii. Quality assurance for typical engineering structures
iv. Nuclear pressure vessels and piping
v. Oil and gas pipelines
vi. Automotive

1.5 Modes of fracture failure

Modes of fracture refers to the decomposition of crack front stresses. A crack front in a structural component is a line usually of varying curvature. Thus, the state of stress in the area of the crack front varies from one point to another. A segment of the crack tip can be divided into three basic loadings or modes [11].

a. Mode I (opening mode)

Mode I also commonly known as the tensile loading's opening phase. In this type of mode, the tensile stress or displacement is normal to the crack surface.

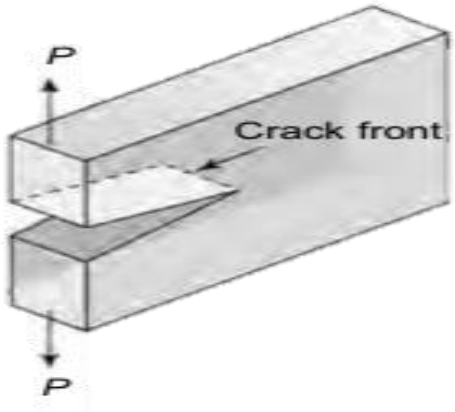

Figure 1- 6 Mode I (opening mode) [3].

b. Mode II (sliding mode)

The shear stress or displacement in this mode is in the plane of the plate; the separation is antisymmetric, and the relative displacement is in the crack front.

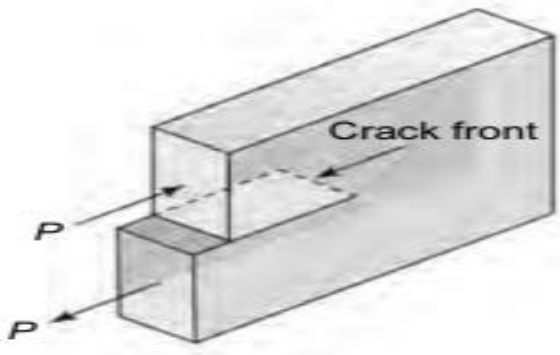

Figure 1- 7 Mode II (sliding mode) [3].

c. Mode III (tearing mode)

The shear stress or displacement is parallel to the crack surface and to the crack front.

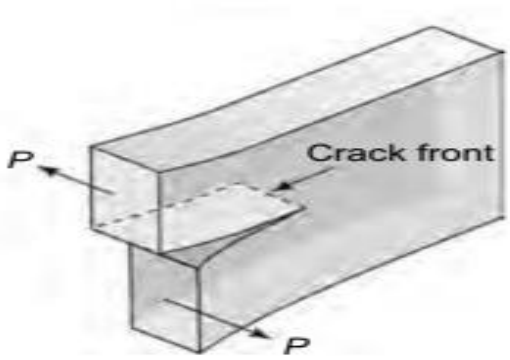

Figure 1- 8 Mode III (tearing mode) [3].

1.6 Notches and stress concentration

A notch is defined as a geometric discontinuity which has a definite depth and root radius. Examples are bolt holes, screw threads or oil holes. The stress at the discontinuity is likely to be significantly greater than the assumed or nominally calculated figure and such discontinuities are therefore termed stress raisers or stress concentrations [12], [13]. By analyzing a plate containing an elliptical hole, Inglis [6] was able to show that the applied stress was magnified at the ends of the major axis of the ellipse (Fig1-9) so that

$$\frac{\sigma_{max}}{\sigma_a} = 1 + \frac{2a}{b} \qquad \text{equation (1- 1)}$$

Where;

σ_{max} : maximum stress at the end of the major axis

σ_a : applied stress applied normal to the major axis

a: half major axis

b: half minor axis

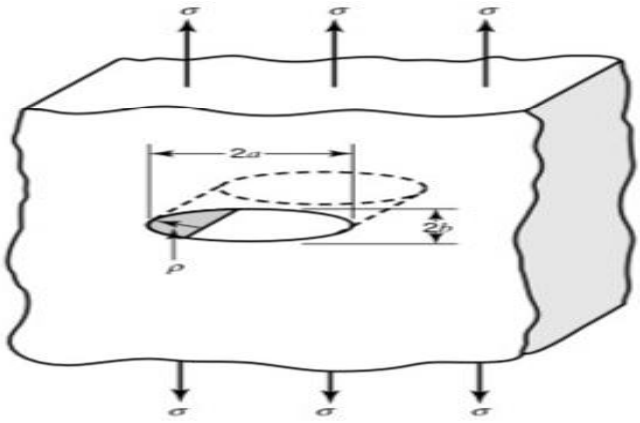

Figure 1- 9 Elliptical hole in infinitely large panel produces stress concentration of 1+2√(a/ρ) [14].

Since the radius of curvature ρ at the end of the ellipse is given by;

$$\rho = \frac{b^2}{a} \qquad \text{equation (1- 2)}$$

Equations (1-1) and (1-2) can be combined to get

$$\sigma_{max} = \sigma_a\left(1 + 2\sqrt{a/\rho}\right) = \sigma_a k_t \qquad \text{equation (1- 3)}$$

The dimensionless ratio $\frac{\sigma_{max}}{\sigma_a}$ is defined as the stress concentration factor k_t, and describes the effect of crack geometry on the local crack-tip stress level.

1.7 Categories of fracture mechanics

Numerous techniques are used to analyze the fracture mechanics issue, each with its own set of parameters. However, two of the forms of fracture mechanics outlined below will be the focus of our study.

1.7.1 Linear-elastic fracture mechanics (LEFM)

LEFM can be applied with parameters like the energy release rate G (energy-based) and the stress intensity factor K (stress-based) [13].

a. Energy release rate G

The energy approach is based on Griffith's [15] postulate;

the extension of a crack that leads to failure occurs when the energy supplied is sufficient to overcome the resistance of the material.

This resistance can be due to surface creation energy, crack tip yield energy, and possibly other types of dissipative energies associated with crack propagation.

Both parameters, energy release rate as well as crack resistance, are important to study the possibility of a crack becoming critical.

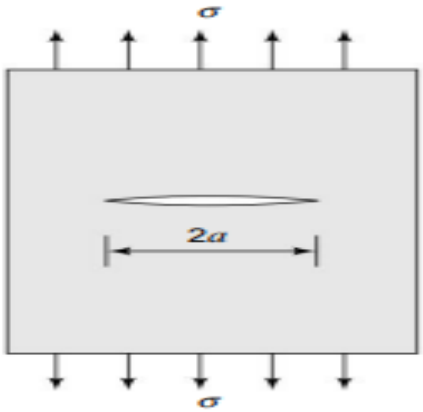

Figure 1- 10 Centre-cracked plate [3].

For a crack of length 2a in an infinite plate subject to a remote tensile stress (Fig1-10), the energy release rate is given by:

$$G = \frac{\pi\sigma^2 a}{E} \qquad \text{equation (1- 4)}$$

Where; E= Young's modulus, σ = the applied stress, a= half crack length.

For linear elastic material, the energy release rate G is defined as the rate of change in potential energy with the crack area, and at the moment of fracture G = G_c, the critical energy release rate, which is a measure of fracture toughness.

$$G \geq \gamma_s = G_c \qquad \text{equation (1- 5)}$$

Where γ_s = the surface energy.

Griffith was the first to propose an energy criterion for the failure of brittle materials, this criterion then extended to ductile materials by other authors (including Irwin [2] and Orowan [16]). They added the energy of plastic deformation in the fracture process (γ_p) to the surface energy introduced by Griffith. Taking into consideration the plastic deformations, the failure criterion is then given in the following form:

$$G \geq \gamma_s + \gamma_p = G_c \qquad \text{equation (1- 6)}$$

Where γ_p is the plastic deformation energy and γ_p» γ_s

b. Stress intensity factor K

Irwin presented an alternative approach, which used a similar mathematical model to that employed by Griffith but based on the analysis of the stress field surrounding a crack in a material subjected to a nominal/biaxial stress. The objective of this approach is to determine the SIF in mode I, taking into account the presence of a plastic zone assumed to be small in comparison to the crack length [3].

Irwin assumes a small crack increase with respect to the size of the plastic zone r_y<< a and considers that the stress σ_{yy} obtained in this zone does not exceed the elastic limit. It is a question of estimating the value r_y for a given value of the stress applied far from σ_{yy}.

For $\theta = 0$, we can write:

$$\sigma_{ys} = \frac{K_I}{\sqrt{2\pi r}} \qquad \text{equation (1- 7)}$$

With,

$$K_I = \sigma_{ys}\sqrt{\pi a} \qquad \text{equation (1- 8)}$$

Irwin considers the existence of a fictitious crack of depth (a + r_y), whose end is located in the center of a plastic zone of radius r at the end of this fictitious notch. The behavior is supposed to be perfectly elastic plastic ($\sigma_y = \sigma$, e = constant inside this zone).

$$r_y = \frac{{K_I}^2}{2\pi{\sigma_{ys}}^2} = \frac{1}{2\pi}\left(\frac{K_I}{\sigma_{ys}}\right)^2 \qquad \text{equation (1- 9)}$$

The analysis is performed by disregarding the non-transmitted forces represented by the hatched area. To take account of these forces, it is necessary to ensure the balance between the two elastic and elastoplastic distributions of stresses. The balance of forces between the two configurations leads to:

$$r_p = 2r_y = \frac{{K_I}^2}{\pi{\sigma_{ys}}^2} \qquad \text{equation (1- 10)}$$

From the value of r_y, Irwin defined the stress intensity factor as

$$K_I = \sigma_{max}\sqrt{\pi(a + r_y)}$$ equation (1- 11)

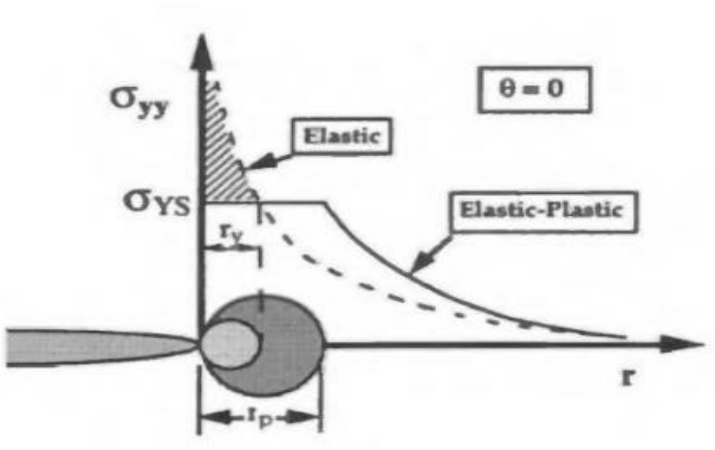

Figure 1- 11 First order and second order estimates of plastic zone size (r_y and r_p respectively) [12].

The cross-hatched area represents load that must be redistributed, resulting in a larger plastic zone.

1.7.2 Elastic-plastic fracture mechanics (EPFM)

EPFM is the theory of fracture, usually characterized by stable crack growth (ductile metals). Three basic methods of EPFM include the crack tip opening displacement (CTOD), the J-integral, and the R-curve methods. However, an in-depth look into the J-integral and the crack tip opening displacement will be conducted [1].

a. J-integral

Like other parameters (G and K), the J-Integral is also a parameter to characterize a crack. In fact, G is a special case of the J-Integral, i.e., G is usually applied only to linear elastic materials, whereas the J-Integral is not only applicable to linear and non-linear elastic materials, but is considered to be very useful to characterize materials, exhibiting elastic-plastic behavior near the crack tip [3]. The J-integral can be regarded as a change of potential energy of the body with an increment of crack extension. The general expression for J, as defined by Rice [17], is given by:

$$J = \int_{\Gamma} (W.d_Y - T.\frac{\partial u}{\partial x}.ds)$$ equation (1- 12)

Where W is strain energy density, T is the component of the traction vector, ∂u is the displacement vector components, ds is the length increment along the contour Γ.

The strain energy density is defined as:

$$W = \int \sigma_{ij} d\varepsilon_{ij} \qquad \text{equation (1- 13)}$$

Where σ_{ij} and ε_{ij} are the stress and strain tensors respectively. The traction is a stress vector at a given point on the contour. That is, if we were to construct a free body diagram of the material inside of the contour, T would define the stresses acting at the boundaries. The components of the traction vector are given by

$$T = \sigma_{ij} n_j \qquad \text{equation (1- 14)}$$

Where n_j are the components of the unit vector normal to Γ.

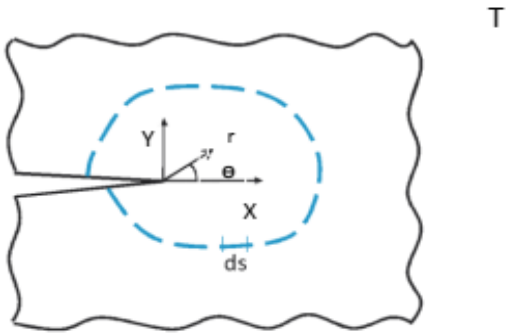

Figure 1- 12 An arbitrary contour around the crack tip used in the definition of J-integral [5].

b. Crack tip opening displacement

CTOD is another parameter suitable to characterize a crack. Unlike parameters G and K, it can be used for both LEFM and EPFM. In 1961 Wells introduced CTOD's approach. This approach focuses on the strains in the crack tip region instead of the stresses, unlike SIF approach. In the presence of plasticity, a crack tip will blunt when it is loaded in tension. Wells proposed to use the crack flank displacement at the tip of a blunting crack, the so-called crack tip opening displacement as a fracture parameter (see Figure 1-14). The CTOD parameter has been found more useful for cracks having large plastic zones [3], [8], [18].

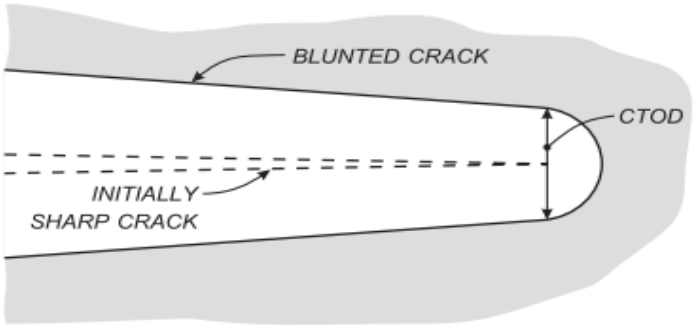

Figure 1- 13 Crack tip opening displacement [8].

1.8 Mechanical constraints

1.8.1 Mechanical stresses and deformations

When a load or a force is applied to a material, this material is subject to a stress defined as the force applied on a unit area. This notion allows us to ignore unit size while considering the effects of force on the physical state of the part. For example, an external force due to gravity is exerted on all materials [19].

a. Stresses

There are 3 types of stresses [19]:

i. Tensile stress tends to stretch a material. Examples include a spring with a weight attached to one end.

ii. Compressive stress that tends to compress a material. Examples include an automobile jack under load.

iii. Shear stress that results from the application of a transverse load. Examples include stress exerted on a shaft that is misaligned.

b. Strain

This is the effect resulting from stress. For example, strain is often measured as the percentage (%) elongation or relative change in length of a part upon which a tensile force has been applied. In many materials, applied stresses can have one or more of the following effects, depending on the magnitude of the stress [19];

When subjected to a relatively low stress, the material undergoes an elastic deformation, and returns to its initial state after the elimination of the stress.

When subjected to moderate levels of stress, the material reaches its elastic limit, or apparent limit of elasticity, and begins to undergo plastic deformation. It will not return to its original state but will undergo permanent deformation.

When subjected to relatively high levels of stress, the material fails or breaks because its conventional limit of proportionality has been exceeded.

1.8.2 Residual stresses

By definition, residual stress refers to a stress distribution, which is present in a structure, component, plate or sheet, while there is no external load applied. In view of the absence of an external load, the residual stresses are sometimes labeled as internal stresses. The background of the terminology “residual stress” is that a residual stress distribution in a material is often left as a residue of inhomogeneous plastic deformation. Residual tensile stress and residual compressive stress always occur together [20].

Residual stresses can be present in a material as a result of different processes. In this section attention is paid to:

i. Inhomogeneous plastic deformation, in many cases at notches.

ii. Production processes.

iii. Shot peening.

iv. Plastic hole expansion.

v. Heat treatment.

vi. Assembling components

1.8.3 State of stresses

One can distinguish two particular stress state: the stress plane state and the strain state. Normally a plane stress approach is applied to members which are relatively thin in relation to their other dimensions, whereas plane strain methods are employed for relatively thick members [21].

a. Plane stress

A plane stress problem is taken to be one in which σ_z is zero. Cases where a uniform stress is applied to the plane surfaces can easily be reduced to this condition by application of a suitable σ_z stress of opposite sign. Shear components in the z direction must also be zero [22].

$$\tau_{zy} = \tau_{zy} = 0 \qquad \text{equation (1- 15)}$$

Plane stress systems are often referred to as two-dimensional or bi-axial stress systems, a typical example of which is the case of thin plates loaded at their edges with forces applied in the plane of the plate.

b. Plane strain

Plane strain problems are normally defined as those in which the strains in the z direction are zero. Again, problems with a uniform strain in the z direction at all points on the plane surface can be reduced to the above case by the addition of a suitable uniform stress sigma σ_z [22].

$$\varepsilon_{zz} = \varepsilon_{yz} = \gamma_{zx} = 0 \qquad \text{equation (1- 16)}$$

A typical example of plane strain is the pressurization of long cylinders where the tri-axiality of the stresses is important.

CHAPTER 2

GENERALITIES ON PIPELINES

CHAPTER 2
GENERALITIES ON PIPELINES

2.1 Introduction

Pipelines have been built in various parts of the world for thousands of years to transport water for drinking and irrigation. The advent of cast-iron pipes in the 18th century boosted the robustness of pipes of all sizes. Steel pipe was invented in the nineteenth century, making it possible to transport natural gas and oil across great distances. Steel pipes had to be threaded together at first, which was difficult for huge pipes. Welding was employed to join pipes in the 1920s, allowing the construction of leakproof, high-pressure, large-diameter pipelines. The majority of high-pressure pipework nowadays is made of steel pipe with welded joints.

2.2 Definition of pipelines

A pipeline is a line of pipes (closed conduit) equipped with pumps, valves, and other control devices for moving liquids, gases, and slurries (fine particles suspended in liquid) [23].

Figure 2- 1 Section of the Trans-Alaska pipeline [23].

2.3 Major components of a pipeline

The major components of an oil and gas pipeline includes;

i. Valves: are mechanical devices that can open or close within the pipeline to control the flow of gas or hazardous liquid.

ii. Flange: connect valves, pipes, and other equipment together.

iii. Fittings: connect segments of pipe or accommodate changes in terrain or direction of the pipe.

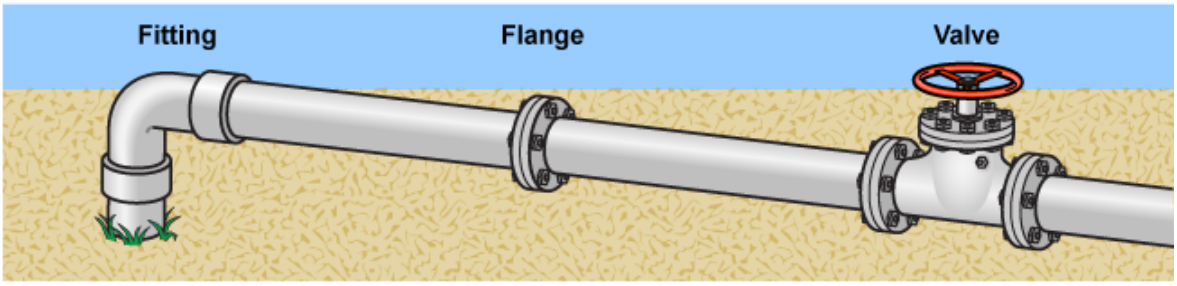

Figure 2- 2 Major components of a pipeline [24].

2.4 Pressure piping

Pressure piping is any piping that carries fluid under internal or external pressure. ASME B31 serves as the design code for piping. All process piping, power piping, pipelines all are examples of pressure piping [25].

i. **High-pressure pipes:** For higher-pressure pipes effect of temperature change has to be considered. If significant temperature changes occur, due to either weather change or cooling following hot welding of a restrained pipe during repair, high stresses can be generated in the pipe to cause the pipe to break, buckle, or bend excessively, or destroy the supports.

ii. **Low-pressure pipes:** For low-pressure pipes, analysis and design are focused on soil properties, soil-pipe interaction, installation (bedding) method, and the rigidity of the pipe.

2.5 Types of pipelines

Pipeline construction involves many different requirements, depending on the application. Thus, pipelines are mainly classified into three categories depending on their purpose or into two categories according to the environment in which they are constructed.

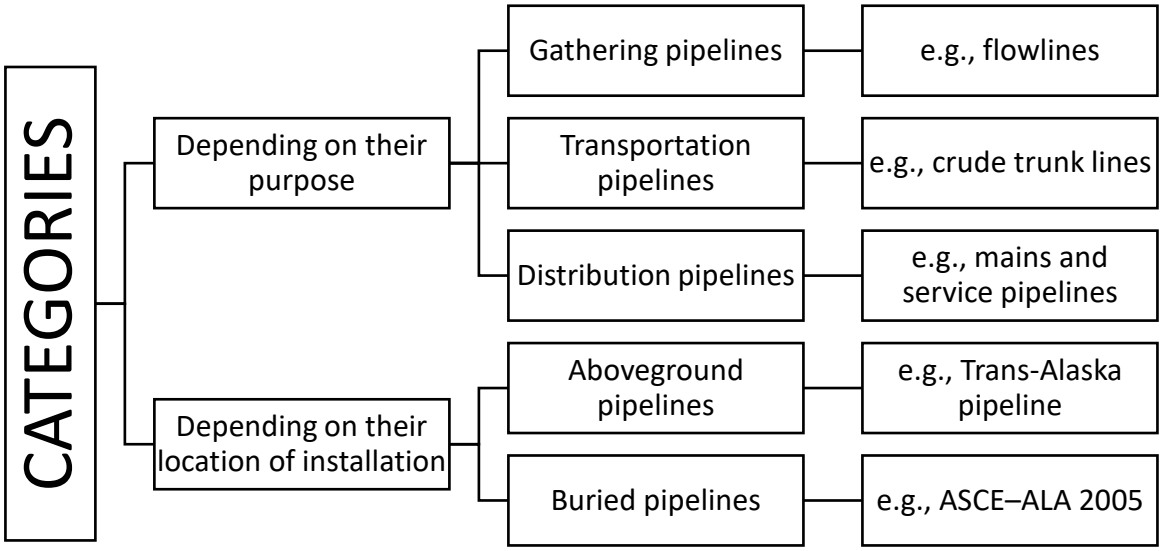

Figure 2- 3 Categories of pipelines.

2.6 Load considerations

Pipelines must be designed for many types of loads, including but not limited to

i. Stress due to pressure generated by the flow (internal pressure)

ii. External pressure by fluid if the pipe is submerged underwater

iii. External pressure is generated by the weight of the earth and by live loads on underground (buried) pipelines.

iv. Loads due to thermal expansion, earthquakes, etc.

2.7 Industrial context

Commercial steel pipes or pipelines are fabricated either by piercing and extruding a hot billet (seamless pipe) or by bending and then welding steel plates or skelp (longitudinal or spiral seam welded pipe). In either case, the fabricator produces a pipe with dimensions (diameter and

thickness) that comply with a standard, such as ASME B36.10 for carbon steel pipe, ASME B36.19 for stainless pipe, or API 5L for line pipe [26].

2.7.1 Design and construction of pipelines

The objective of pipeline design and engineering is to route, design, and construct a pipeline that can operate safely with minimal impact on the environment, and one that is cost-effective both in terms of capital and operating costs. To achieve this objective, sophisticated engineering and economic studies are necessary to optimize variables such as a pipeline routing, size (diameter), materials, and compression and pumping requirements [27].

Construction of pipelines involves route survey, ditching or trenching, transporting the pipes, fittings, and other materials to the site, stringing the pipes along the ditch, bending steel pipes in the field to suit local topography, applying coating and wrapping to steel pipes, joining pipes together either before or after they are lowered into the trench, checking for possible welding flaws or leakage at the joints and then covering the trenches by soil and restoration of the land to its original appearance [23].

The major factors influencing the design and construction of pipelines are listed here.

i. Nature of fluid being transported (gas or liquid) and fluid properties.

ii. Volume flow rate.

iii. Length of the pipeline.

iv. Terrain and medium (soil/water) traversed by the pipeline.

v. Climatic conditions – extreme heat/cold.

vi. Codes, standards and regulations governing the design, construction and operation of the pipeline.

vii. Economics.

viii. Materials.

ix. Construction, operation and maintenance of the pipeline

2.7.2 Materials

The selection of a pipeline material type should be determined at the conceptual design stage, with metallic, especially carbon steel, being the most commonly used materials. Figure (2-4) shows some of the materials used in the construction of pipelines.

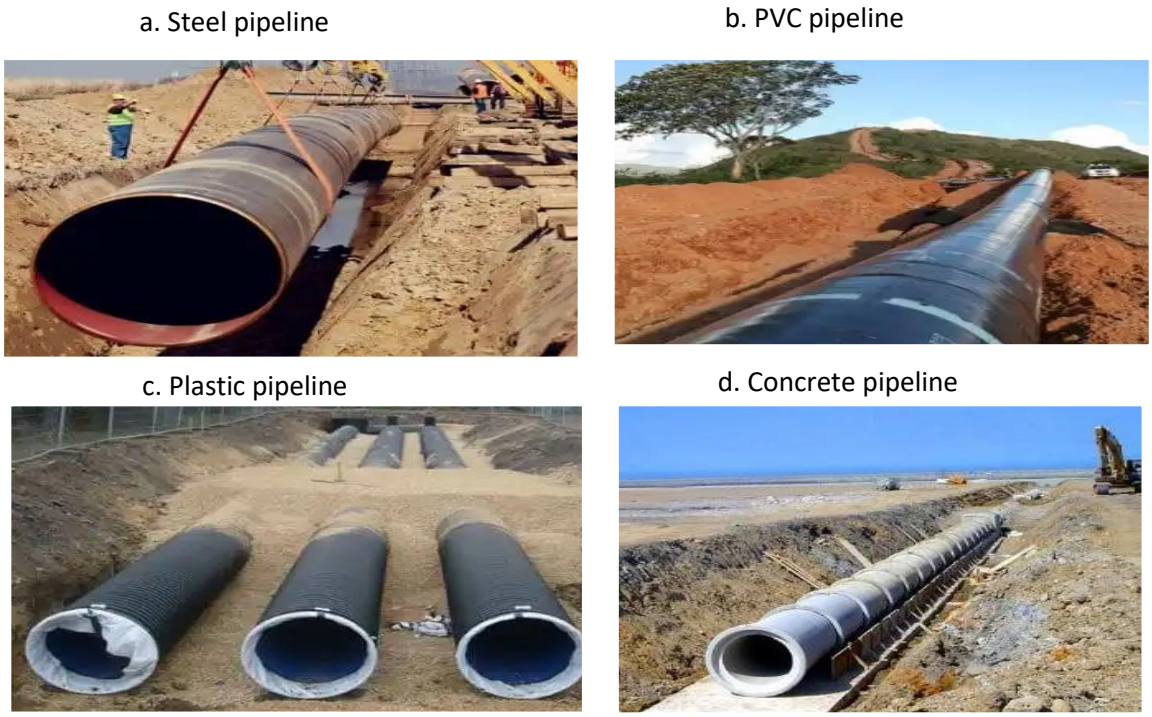

Figure 2- 4 Examples of some pipeline [28].

2.7.3 Weldability

Weldability is the capacity of a material to be welded and achieve the required properties without introducing defects.

2.7.3.1 Welding

Pipe welding is a method for joining two pipes together. Welding techniques used for pipes include arc welding processes (Metal Inert Gas welding and Tungsten Inert Gas welding). Pipeline welding should conform to the relevant ASME codes like B31.4, B31.8, BPVC, etc [29].

Figure 2- 5 Pipeline welding [30].

The following are the 5 main types of welding joints:

i. Butt joint welding

ii. Lap joint welding

iii. Edge joint welding

iv. Tee joint welding

v. Corner joint welding

2.7.3.2 Butt joint welding

This type of weld is used when the members are in same plane. Butt weld is also termed as groove weld. The butt weld is used to join structural members carrying direct compression or tension. It is used to make tee-joint and butt-joint. For the examination of elliptical cracks in pipelines with a thickness transition, this method of welding as shown in (Figure 2-6e) is utilized in this study. Below is the acceptable design for unequal wall thicknesses according to ASME B31.8 [31].

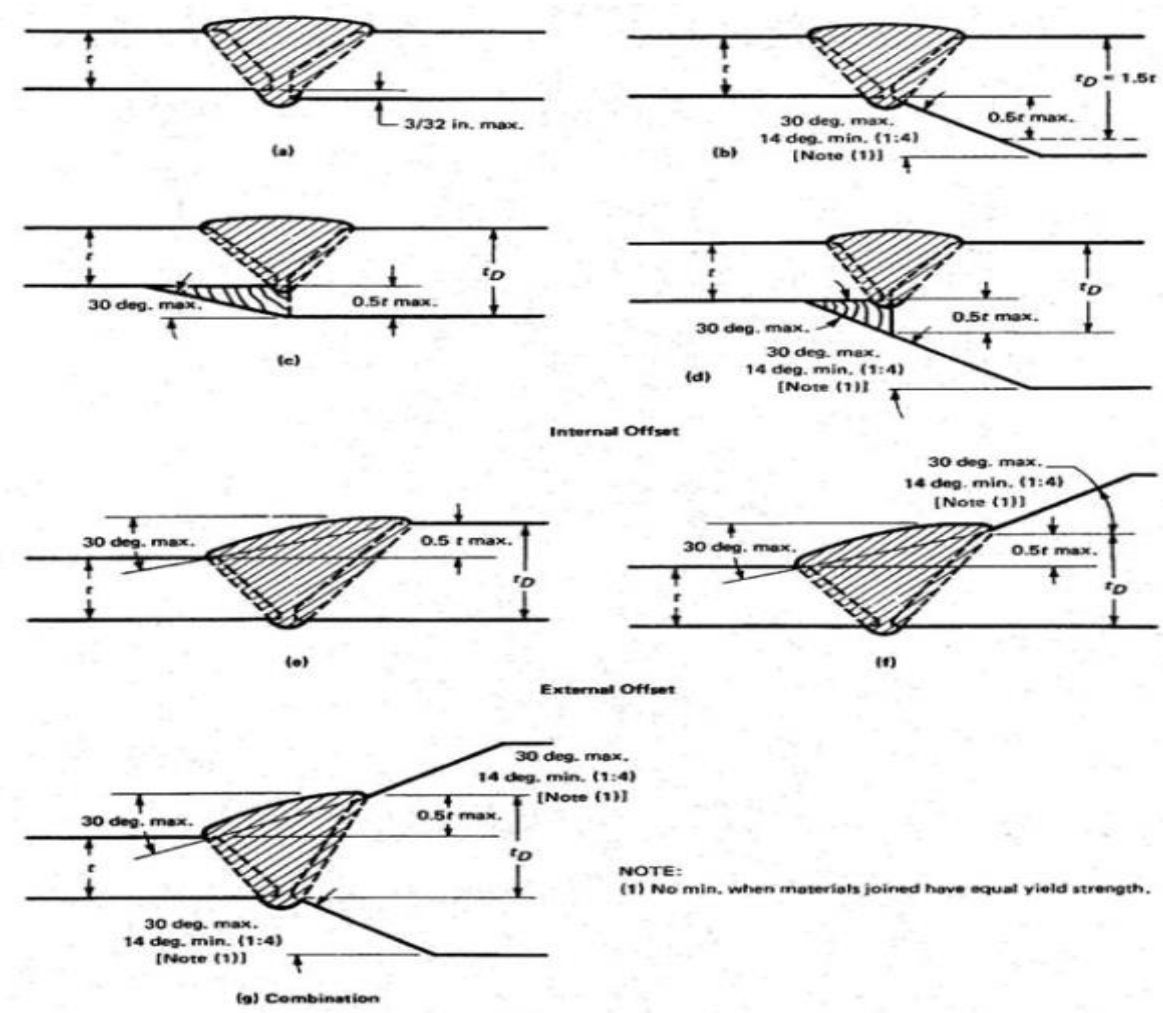

Figure 2- 6 Acceptable design for unequal wall thickness [32].

2.7.3.3 Pipeline welding process selection

Pipeline welding is the backbone of pipeline construction. Hence, the pipeline welding process selection must be done, considering various factors as mentioned below:

i. Pipeline material

ii. Pipe diameter and wall thickness

iii. Welding location

iv. Weldment properties

v. Welding direction (uphill or downhill)

vi. Welding quality

vii. Economic consideration

viii. HSE consideration

2.7.3.4 Types of welding process

The sources of heat for welding include electric arc, electric resistance, flame, laser, and electron beam [33].

i. **Shielded metal arc welding (SMAW):** The heat for this process is provided by an electric arc that melts a consumable electrode, with some of the metal being welded. When the weld metal cools, it hardens to form the weld.

ii. **Submerged arc welding (SAW):** In this process, joining involves creating an electric arc between an electrode and welded workpiece, with a powdered flux blanket providing electrical conduction when molten.

iii. **Gas-metal arc welding (GMAW):** This process also uses the heat from an electric arc. The arc is covered by an inert gas, such as argon or helium. The insert-gas-shielded metal arc process uses a consumable, continuous electrode.

iv. **Gas-tungsten arc welding (GTAW):** An inert gas shield is required when welding with tungsten electrodes using the gas-tungsten arc welding process.

v. **Electric resistance welding (ERW**): Is a process by which metals can be joined together by applying pressure and conducting a strong electric current to melt and forge them.

2.8 Manufacturing process of pipeline tubes

They are primarily made using two different manufacturing processes that create either welded pipes (SAW and ERW) or seamless pipes (SMLS). The raw steel is initially cast into a more workable start form (hot billet or flat strip) in both manufacturing processes.

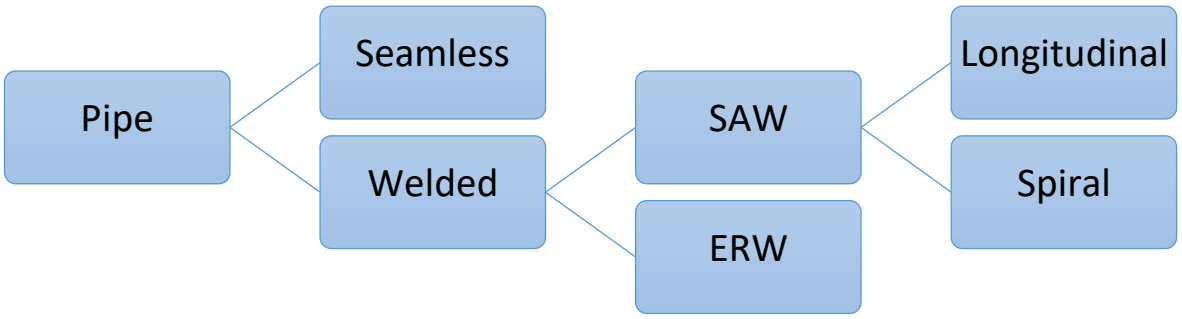

Figure 2- 7 Manufacturing processes of pipeline tubes or pipes.

2.8.1 Seamless tube or pipe

A seamless tube is a solid metal tube with threads at one or both ends that can be threaded to another hollow tube or pipe without any welding seam. The presence of any seam on a welded tube acts as a weak point, however if the tube is seamless, it tends to be solid and overcome various industrial forces and pressures while in operation [34].

The seamless fabrication process follows several steps, depending on the applicable material specification. These steps typically include the operations shown in Figure 2-7.

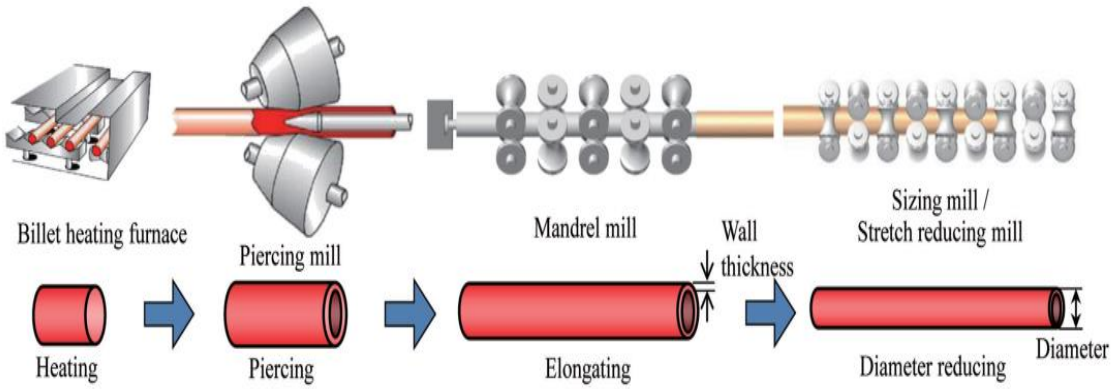

Figure 2- 8 Schematic of Mannesmann process in seamless pipe production [35].

2.8.2 Welded pipe

The term "welded pipe" refers to a tubular product created from flat plates, or "skelp," that have been shaped, bent, and prepared for welding. A longitudinal seam weld is the method used most frequently for large diameter pipe.

2.8.2.1 SAW

These pipes are manufactured from plates, normally rolled and seam-welded together. There are 2 types of submerged arc welding processes, namely:

a. Longitudinal submerged arc welding (SAW)

In LSAW process, longitudinal edges of steel plates are first beveled using carbide milling equipment. Beveled plates are then formed into a U shape using a U-press and subsequently into an O shape using an O-press. Figure 2-9 describes briefly the longitudinal submerged arc welding manufacturing processes [36].

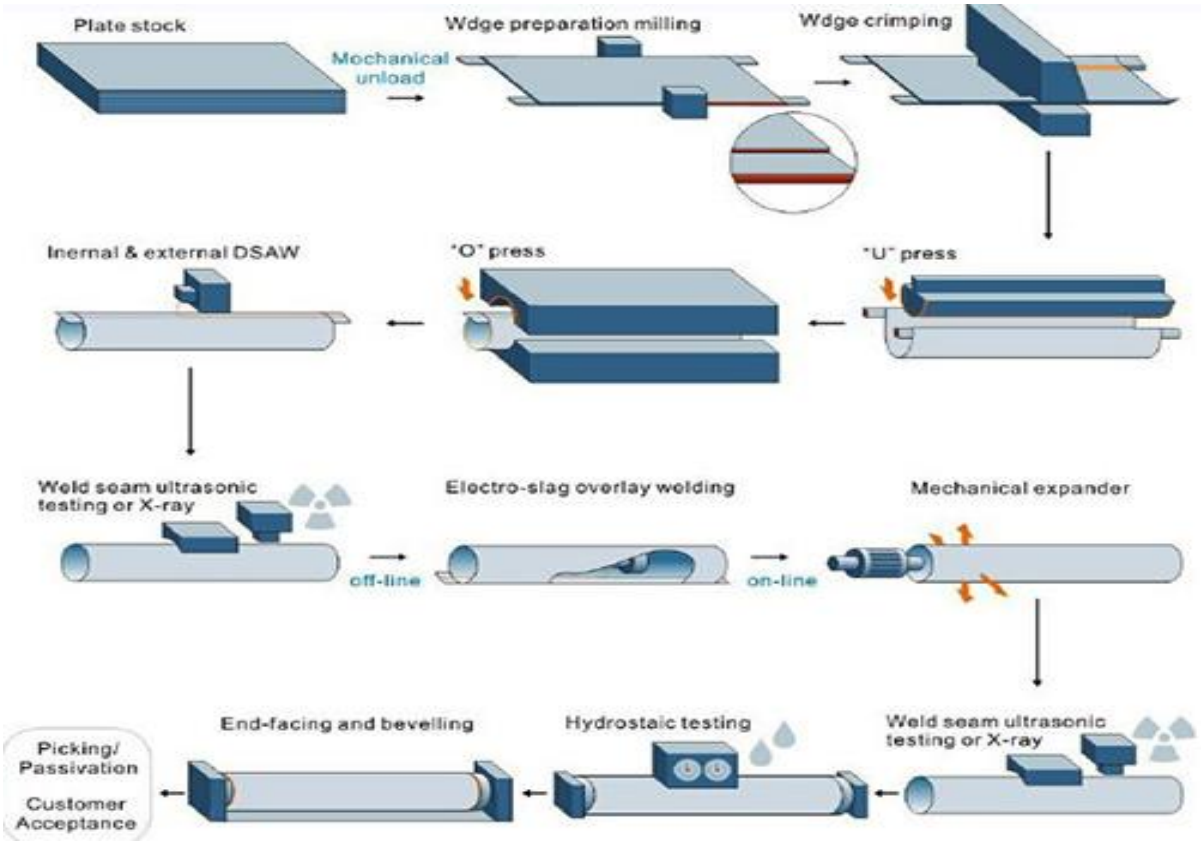

Figure 2- 9 Longitudinal submerged welded (LSAW) [37].

b. Spiral submerged arc welding (SSAW)

A helix-shaped welding line is produced by the spiral submerged arc welding (SSAW) method. It employs the same submerged arc welding with LSAW pipe technology. The only significant distinction is that SSAW pipes are spiral welded, whereas LSAW pipes are longitudinally welded. The steel strip is rolled throughout the manufacturing process such that the rolling

direction forms an angle with the direction of the pipe center, followed by shaping and welding, resulting in a spiral-shaped welding seam (see Figure 2-10).

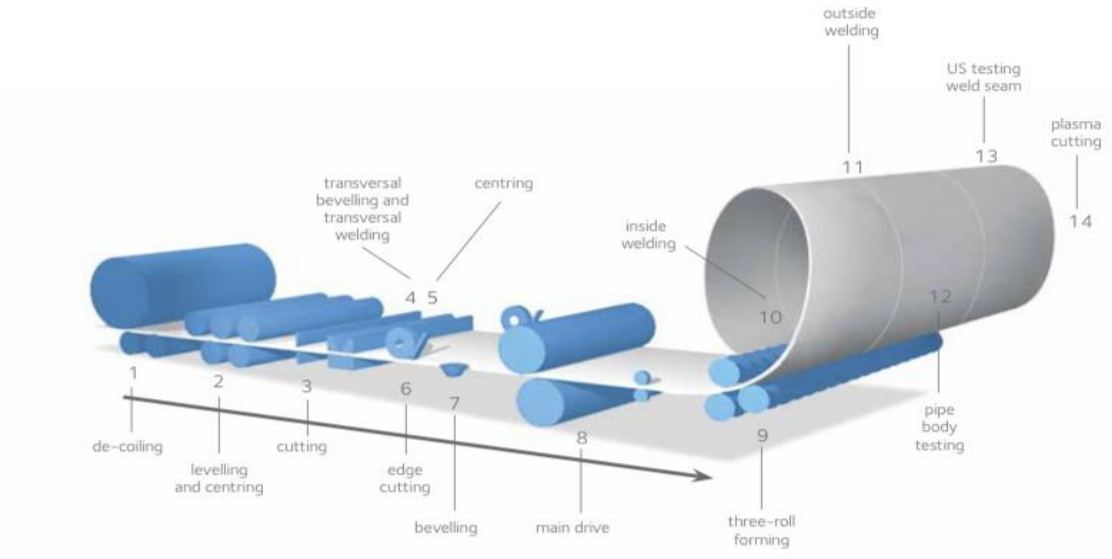

Figure 2- 10 Spiral submerged arc welding (SSAW) process [35].

2.8.2.2 Electric resistance welding (ERW)

In electric resistance welding (ERW) process, a flat sheet of steel is cold formed into a cylindrical shape to create pipe. The steel is then heated to a degree at which the edges of the steel cylinder are pressed together to establish a bond without the use of welding filler material.

Several electric resistance welding (ERW) processes are available for pipe production. The two main types of ERW are:

i. High frequency welding

ii. Rotary contact wheel welding

2.9 Major causes of pipeline failures

Damage due to corrosion, mechanical damage, and third-party interference or errors are the three main causes of pipeline failure. Weld defects, material defects, and fitting defects are caused by irregularities during construction and repair. Pitting (point corrosion) and uniform corrosion both include the regular and uniform loss of metal from the pipeline's corroding surface.

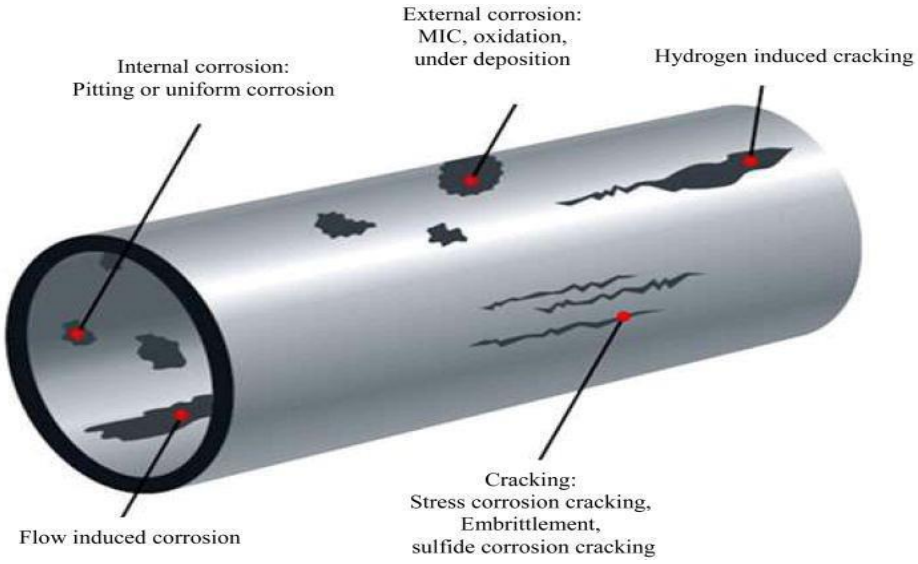

Figure 2- 11 Some of the major causes of pipeline failures [38].

2.9.1 Corrosion

Pipeline corrosion is the breakdown of the pipeline or its mechanical characteristics due to the nearby environment, which may include the earth, the atmosphere, water, or other fluids. Corrosion is a tremendously complex phenomenon because of the vast number of variables involved in the electrochemical process. The primary chemical components that cause corrosion reactions to occur in pipelines are oxygen, acidic Sulfur, and acidic chloride that dissolve in the water pipeline. In all cases of corrosion, the electrolyte must be present for the reaction to occur. The following are some of the types of corrosion;

i. Uniform pipe corrosion

ii. Microbiologically induced corrosion (MIC)

iii. Pitting corrosion

2.9.2 Cracking

A crack is a type of failure whereby fracture lines are formed on the circumference and/or along the length of the piping. Cracks are predominantly formed in rigid pipes and can be a precursor to pipe rupture or breakage. There are numerous types of cracking, all brought on by various mechanisms (see Figure 2-12). Some of the types of cracks are discussed below [39].

Figure 2- 12 The various types of cracks [40].

a. Fatigue cracks

This type of cracking is associated with dents, seam weld flaws and other areas of stress concentration. Fatigue cracks grow in response to pressure cycling or stress and are aligned at right angles to the principal stress [41].

b. Weld cracks

Hot cracks and cold cracks are the two primary forms of cracks that arise in and around fusion welds in the weld metal. The term "hot crack" refers to a fracture that forms during cooling, and the term "cold crack" refers to a crack that forms later.

c. Stress corrosion cracking (SCC)

SCC is a form of Environmental Assisted Cracking (EAC). SCC refers to crack propagation due to an anodic reaction at the crack tip. The crack propagates because the material at the crack tip is consumed by the corrosion reaction [42].

Two main types of SCC are:

i. **High pH stress corrosion cracking (SCC):** this type of cracking occurs on external pipe surfaces, such as locations of coating disbanding.

ii. **Near-neutral pH stress corrosion cracking (SCC):** this type of cracking occurs in freely corroding conditions. The cracking is transgranular in nature, propagating through pipe wall thickness.

d. Sulphur stress cracking (SSC)

Hydrogen sulfide (H2S), which naturally occurs in natural gas and oil, is present in small amounts. In chloride-containing settings, SSC can happen in conjunction with elevated temperatures and pressure. These circumstances typically arise during the production of oil and gas, primarily offshore.

e. Hydrogen induced cracking

HIC is a materials and corrosion-related problem that occurs in surface production systems. Steels used to construct sour-gas production facilities and flowlines may corrode from wet hydrogen sulfide gas in the production steam. The corrosion process generates hydrogen that may dame the steel, resulting HIC and other forms of damage from hydrogen [43].

2.9.3 Mechanical damage or defects

Around the world, pipeline failures are most frequently caused by mechanical damage. It can happen when a pipeline is hit from above, or when rocks or soil are moved beneath.

a. Dent

A dent is defined here as a depression that resulted from contact with an object outside the pipe and generated a significant change in the curvature of the pipe wall, leading to plastic deformation of the pipe wall [44].

Figure 2- 13 A dent on a pipe [44].

b. Gouges or scratches

A gouge is described as surface damage to a pipeline brought on by contact with a foreign object that has moved or removed material from the pipe, causing metal loss, metal movement, microstructure damage, cracking, and/or the creation of a harmful feature as a result of the damage process [41].

Figure 2- 14 A gouge or a scratch [44].

c. Combined defect

It is best to proceed cautiously when dents and gouges are discovered together, contain cracks or broken metal, or are located close to a seam or girth weld.

2.10 Pipeline integrity

Pipeline integrity is the concept of safeguarding pipelines and related components to ensure they are free from damage or defect, which prevents harmful chemicals from being released from the pipeline into the nearby environment.

2.10.1 Pipeline integrity management (PIM)

PIM is a series of efforts aimed at ensuring the integrity of pipelines. PIM allows operators to assess locations on a pipeline that are most vulnerable to corrosion and the time to failure due to the corrosion rate. ASME B31.8S (managing system integrity of gas pipeline) provides information necessary to develop and implement an effective integrity management [45].

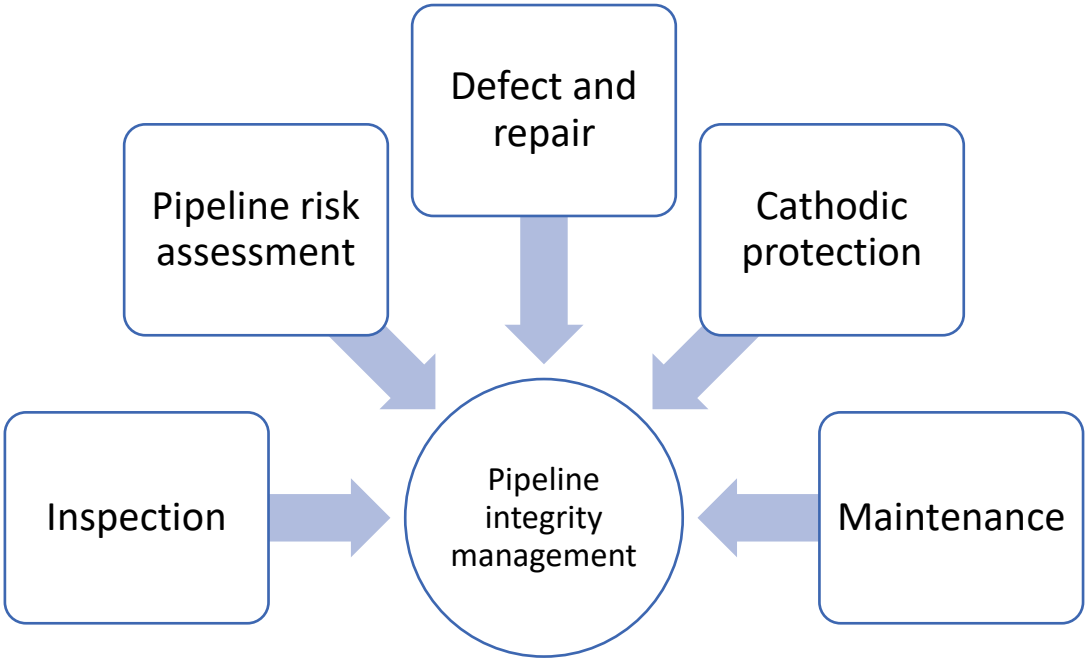

Figure 2- 15 Sectors of a pipeline integrity management.

2.10.2 Pipeline inspection

Inspection pigs, also referred to as smart pigs, learn details about the pipeline from within. Temperatures, pressure, corrosion/metal loss, cracks, weld flaws, and other data are the kind of information that inspection pigs collect. Three different sorts of specialized smart pigs have developed: metal loss tools, fracture detection tools, and geometry tools.

a. Metal loss tools

i. Magnetic flux leakage (MFL): is a method of pipeline inspection that involves injecting magnetic flux into the pipe's walls in order to find leaks, corrosion, or other problems.

ii. Ultrasonic (UT): This method uses ultrasonic noises to inspect the pipeline by timing how long it takes an echo to return to the sensor.

b. Crack detection tools

i. Ultrasonic crack detection: involves sending an ultrasonic signal into the pipe wall, which is then reflected off the pipe's interior and exterior surfaces. The signal bounces back along the tool's path if a crack is found.

ii. Transverse field inspection (TFI): This method uses magnetic flux leakage to create a flux field around an object to detect cracks, such as corrosion along longitudinal seams and cracks in those seams.

iii. Elastic wave tool: To find and size longitudinally oriented cracks and manufacturing problems, this developing device sends ultrasounds in two directions along the pipeline.

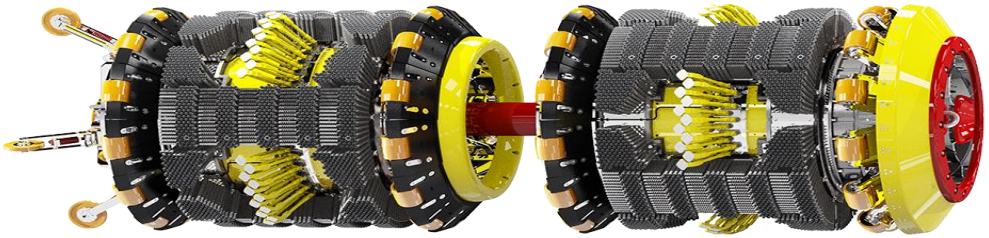

Figure 2- 16 Transverse field inspection tool [46].

c. Geometry tools

The aim of geometry tools is to obtain data regarding the geometry, or physical form, of a pipeline.

i. Caliper tools: is designed to record geometry or condition of the pipeline such as dents buckles, wrinkles, ovality, bend radius and angle, etc. [47].

ii. Pipe deformation tools: This device works similarly to a caliper, but it also uses gyroscopes to display the dent or deformation in the pipe at the hour mark.

2.10.3 Pipeline risk assessment

Risk assessment is a predictive technique, usually making use of historical data, modeling, assumptions and expert judgement and as such there is always a degree of uncertainty in the risk estimates. Risk assessment can be either qualitative or quantitative:

i. Qualitative (e.g., assessing likelihood and consequences using scales from ‘very low’ to ‘very high’)

ii. Quantitative (e.g., assessing likelihood in terms of annual frequencies of occurrence and estimating consequences in terms of specific numbers of casualties)

Risk management uses the results of risk assessments to consider of whether enough precautions have been taken or whether more should be done to prevent harm, often utilizing cost benefit analysis to examine the cost of alterative risk reducing measures.

The following are some of the risk assessment methods

i. Risk tolerability criteria

ii. Risk control hierarchy

2.10.4 Defects and repair

When a flaw or anomaly in a pipeline is found that jeopardizes the pipeline's integrity, a repair must be undertaken utilizing methods that return the pipeline to its original design specifications. Several methods can be used to remediate pipeline defects and anomalies, these include [48]:

Removal and replacements of pipe is done by the following methods:

i. Filet welded patch: this method can be used to repair pressure vessel temporary by placing a patch plat cover on damaged areas and then welded to the vessel by filet weld.

ii. Half repair sleeves: sleeves are the most important and widely used method of repair of pipeline defects. Sleeves may be steel, type A (reinforcement), type B (pressure-retaining reinforcement), or composite material.

iii. Weld overlay/weld deposition repair: is a pipeline repair technique where a suitable metal is deposited through welding to the pipe surface, valve body/trim, or a pipe fitting in the form of a layer.

2.10.5 Maintenance

Maintaining a pipeline's integrity and functionality entails taking care of all of the related parts. This is known as pipeline maintenance. This task should not be performed only once because regular, thorough maintenance will prolong the pipe's life and reduce the risk of failure. Cleaning is a routine maintenance procedure carried out on pipelines in all sectors. Pipe cleaning is frequently a prerequisite for carrying out a piping examination [47].

a. Visual inspection

b. jettyrobot

Figure 2- 17 Jettyrobot in an inspection and cleaning process [47].

2.10.6 Cathodic protection

Cathodic protection is a common method used in various industries that uses a low electrical current to prevent corrosion of metal structures such as pipelines, tanks, steel-pier piles and offshore oil platforms [49].

A cathodic protection system is designed in accordance with regulatory requirements and pipeline industry codes and practices giving consideration to:

i. Length of pipeline to be protected

ii. Thickness of the pipeline coating

iii. Soil characteristics including

   a. Type of soil (i.e., sand, clay, loam)

   b. Corrosive nature of soil

   c. Soil resistance to passage of electrical current

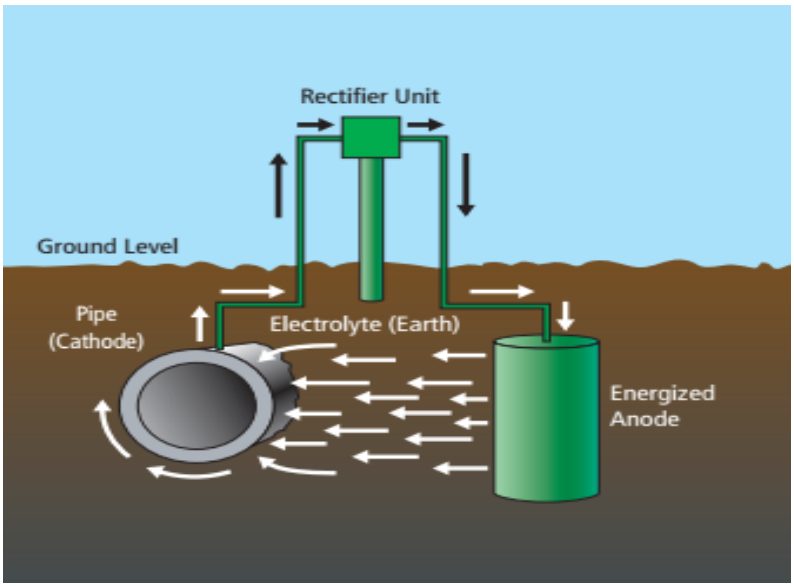

Figure 2- 18 Cathodic protection setup [49].

In essence, cathodic protection connects the base metal at risk (steel) to a sacrificial metal that corrodes in place of the base metal.

CHAPTER 3

MODELING AND SIMULATION OF A CRACKED PIPELINE AND ANALYSIS OF RESULTS

CHAPTER 3

MODELING AND SIMULATION OF A CRACKED PIPE AND ANALYSIS OF RESULTS

3.1 Introduction

The numerical simulation discussed in Chapter 3 deals with the various fracture shapes, their locations, types of loading, and scratches that can occur on a pipeline.

As previously illustrated in figure 2–6, thickness transitions seen in industry are divided into two forms: single slope transitions and double slope transitions. The instance of a single slope transition is the subject of our investigation, and the acceptable design for a single slope transition for unequal wall thicknesses that we used as per ASME B31.8 [48] is shown below.

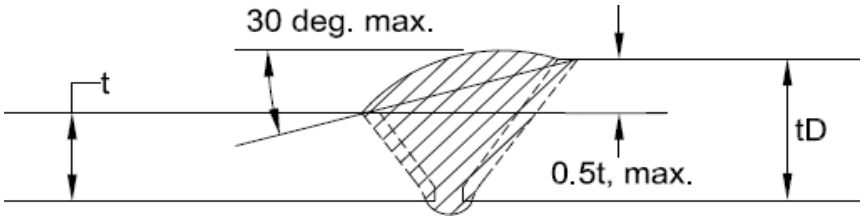

Figure 3- 1 Acceptable design for a single slope transition according to ASME B31.8 [48].

The objective of this chapter is to investigate the fracture behavior of a pipeline with an elliptical crack and scratch using the stress intensity factor in Mode I (K_I).

3.2 Presentation of the Abacus/CAE software

ABAQUS/CAE is a complete Abaqus environment that provides a simple, consistent interface for creation, submitting, monitoring, and evaluating results from Abaqus/Standard and Abaqus/Explicit simulations. Abaqus/CAE is divided into modules, where each module defines a logical aspect of the modeling process; for example, defining the geometry, defining the material properties, and generation a mesh. As you move from module to module, you build the model from which Abaqus/CAE generates an input file that you submit to Abaqus/Standard or Abaqus/Explicit analysis product. The analysis product performs the analysis, send information to Abaqus/CAE to allow you to monitor the process of the job, and generates an output database. Finally, you use the Visualization module of Abaqus/CAE (also licensed separately as Abaqus/Viewer) to read the output database and view the results of your analysis. Abaqus/Viewer provides graphical display of Abaqus finite element models and results [50].

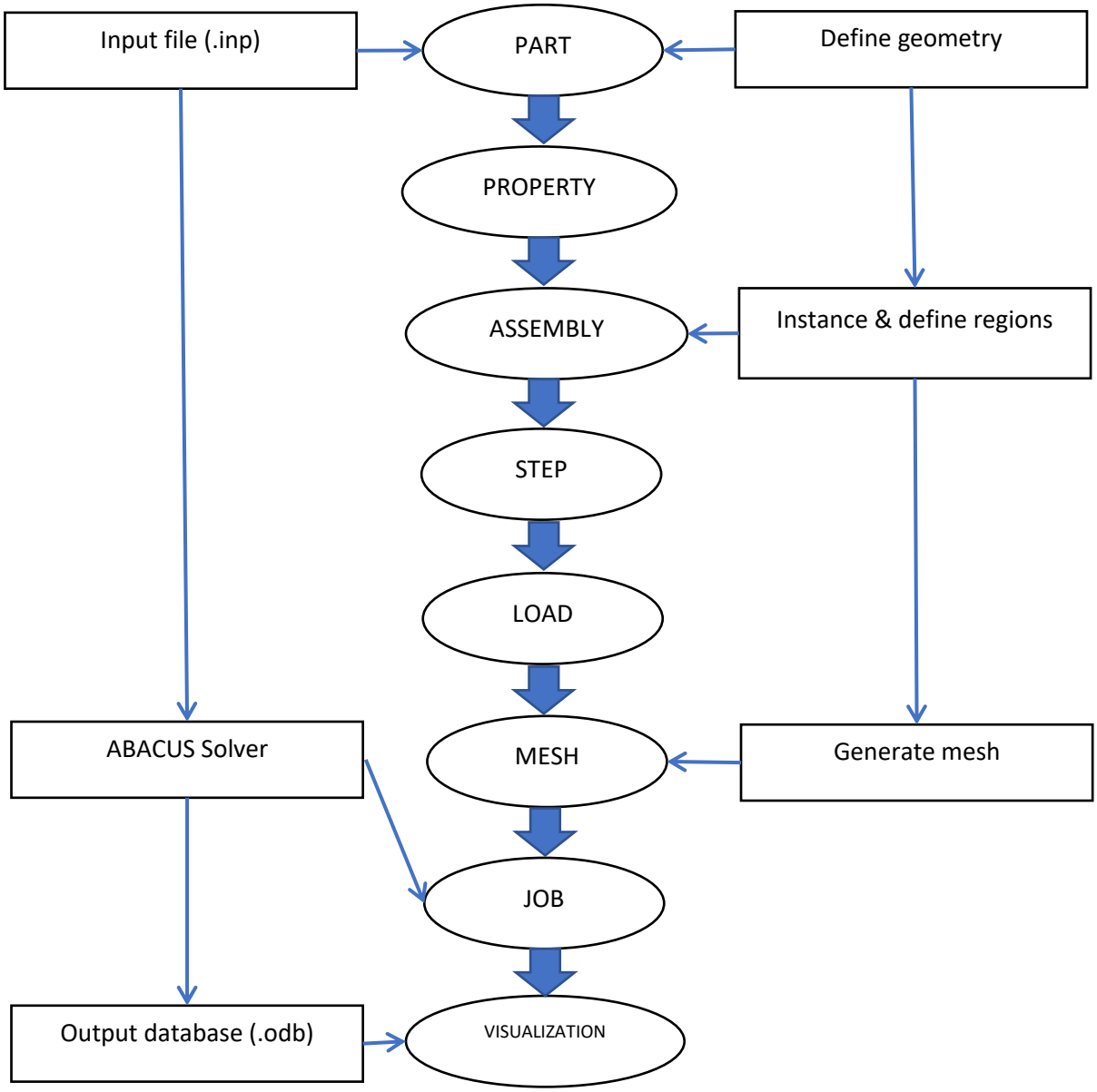

Figure 3- 2 Steps to follow in the programming [51].

In the Abaqus calculation code, the data file describes the geometries, the materials, the boundary conditions with an extension (.inp) and the results file describes the contours and the result curves with the extension (.odb) [51].

As depicted in figure 3-1 above, Abaqus' computation process includes the following modules:

3.2.1 Part module

Using the ABAQUS geometry drawing feature, the Part module enables us to build and edit individual pieces. The geometric model of the pipeline under study is shown in Figure 3-2, and its geometric characteristics are shown in the table below.

Symbol	Value(mm)	Description
t	12.7	Thickness of the thinner pipe
t_D	19.05	Thickness of the thicker pipe
x	11.14	Horizontal length of the transition zone
Ri	165,1	Interior radius of pipe
Re	177,8	Exterior radius of thinner pipe
Lp	1000	Length of pipe

Table 3- 1 Geometric characteristics of the pipeline.

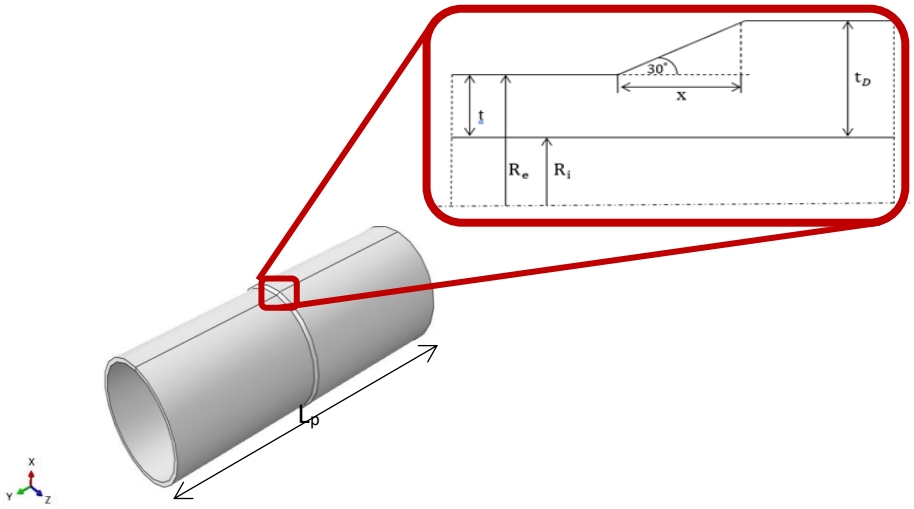

Figure 3- 3 Geometry of the pipe.

3.2.2 Property module

This module assigns the material definitions and material characteristics for each region of the parts. The pipe under study is made of API 5L X65 steel and its mechanical properties are summarized in Table 3-2 below. We assigned only the Young modulus and the Poisson's ration of our material in this module. The material model is considered elastic.

Young modulus (GPa)	**205**
Poisson's ratio	0.3
Minimum yield strength (MPa)	415

Table 3- 2 Mechanical properties of API 5L X65 steel [52].

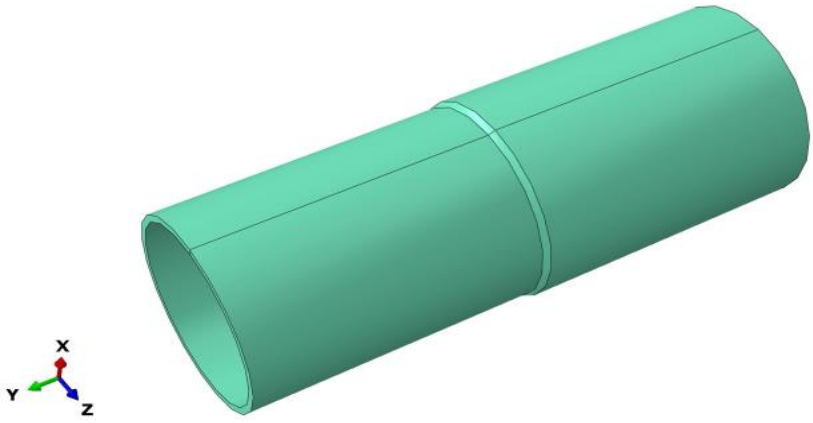

Figure 3- 4 Properties of the pipe.

3.2.3 Assembly module

Using a global coordinate system, this module was used to build instances of the parts and assemble the parts (pipe, crack disk, and scratch shell) in relation to one another.

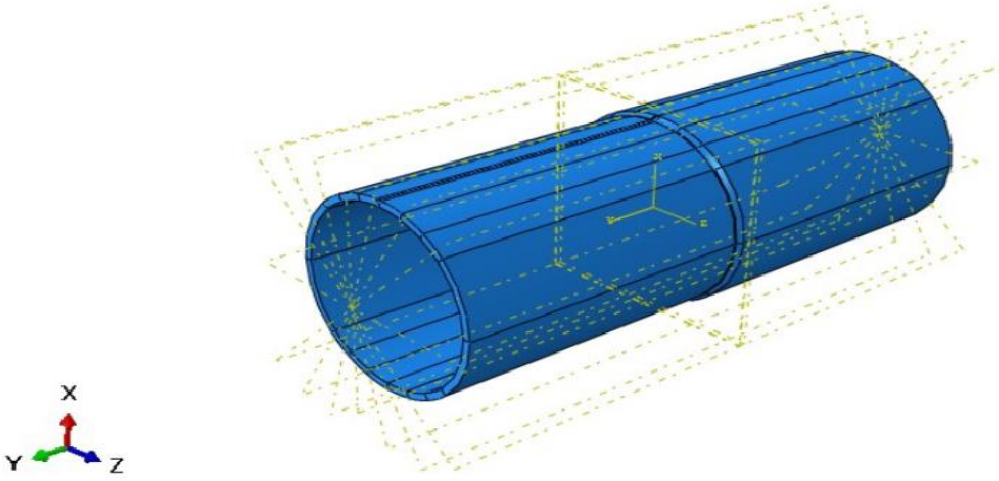

Figure 3- 5 Assembly of different parts created in module part.

3.2.4 Step module

In this module the output request of our study is defined, for our study the calculation of the stress intensity factor with "Maximum tangential stress" is requested in the sub-module 'OUTPUT HISTORY'. The number of contours set is 5 and the nature of the calculation is static general.

3.2.5 Interaction module

This module is used to specify connections between two points, two edges, or a point and a surface, as well as mechanical and thermal interactions between model regions.

In this module we assigned our seam and then used the contour integral option to compute the crack propagation direction " Normal to plane" at initiation when the SIFs are evaluated.

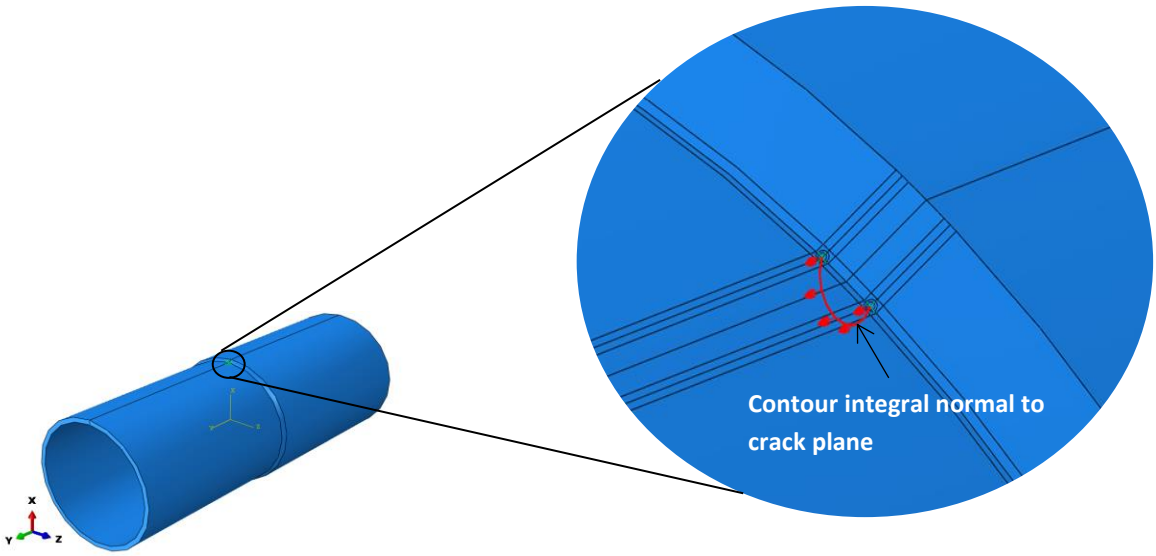

Figure 3- 6 Declaration of interactions.

3.2.6 Load module

The model's loads and boundary conditions are specified using this load module.

In our study, the pipe is subjected to an internal pressure of P=70 Bar=7MPa and one of the two faces of the plane is blocked along the Y axis ($u_y = 0$) while the other has a displacement of U_y = - 0.5mm in the Y axis.

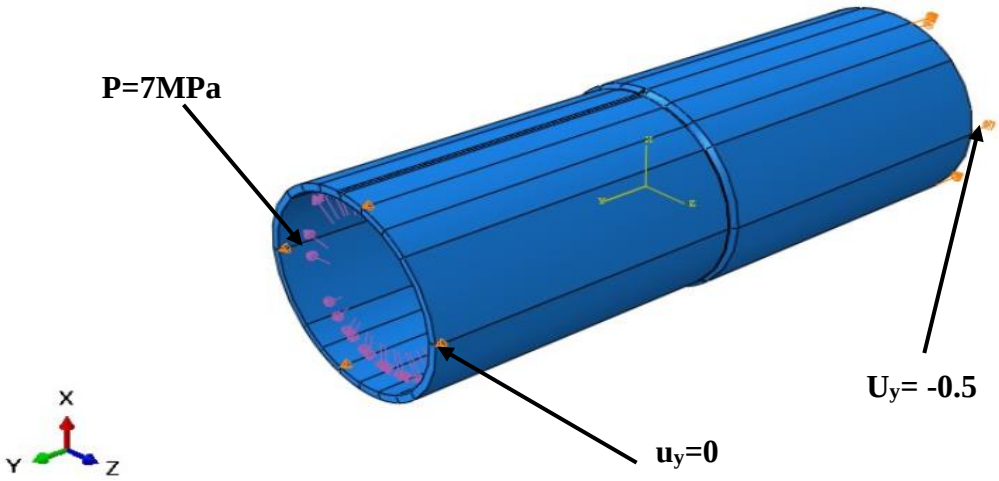

Figure 3- 7 Boundary conditions.

3.2.7 Mesh module

The mesh module defines seeding, mesh controls, algorithms, and element kinds so as to create a finite element mesh on an assembly.

In our assembly, the mesh is of the C3D20R structured quadratic type. The crack in the pipeline leads to a geometric singularity causing a stress concentration. Therefore, a refined mesh is made around the crack where the size of the elements in the vicinity of the crack face is 0.05mm. The total number of elements in the cracked pipe structure is 47146 and for a cracked pipe with a scratch is 47474.

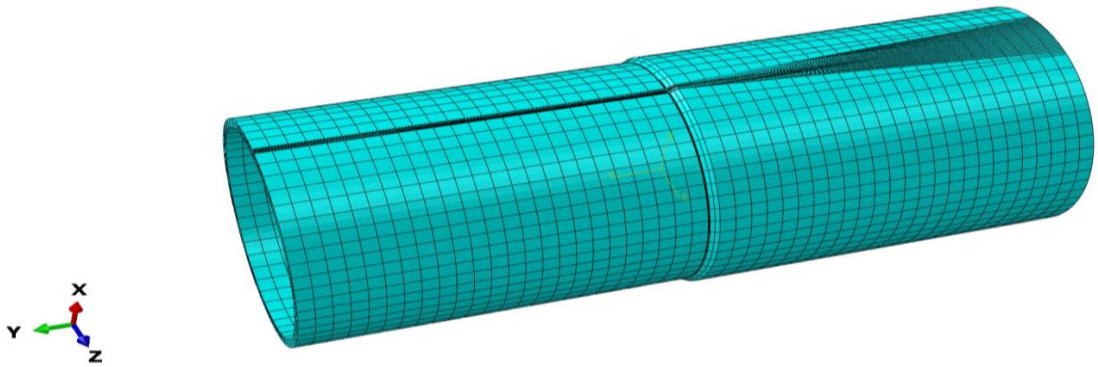

Figure 3- 8 Mesh of the geometric model.

3.2.8 Job module

The job module, which will submit a job for analysis and track its progress, is then used in the following phase to complete the analysis once all of the model's modules have been determined and defined.

3.2.9 Visualization module

This module is used to present finite element models and results graphically. It is under this module where we can find animated analyses of deformed forms, contours, graphs, and other data.

3.3 Schematic geometry of the crack

The non-dimensional ratios a/c and a/t, where a and c are the crack's depth and semi-length, respectively, characterize the various crack geometries under consideration. In our study of the elliptical crack, the ratio a/c is a constant (a/c=1) thus making our crack circular. The crack

front is symmetric and consists of the surface points (S_0 and S_{100}), and the deepest point labelled D.

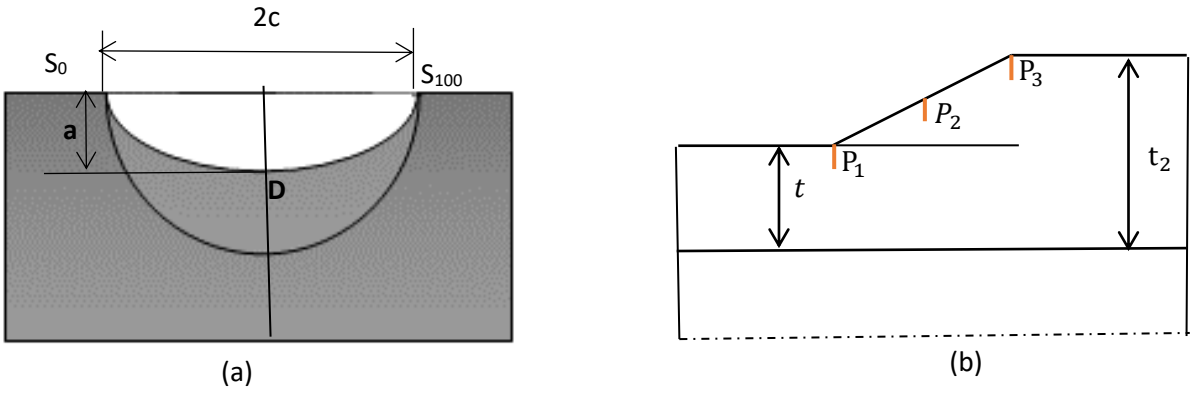

Figure 3- 9 Elliptical crack's (a) geometry (b) various positions along the transition zone.

The following positions along the transition zone (figure 3-9b) are where elliptical cracks are expected to be found:

P_1: is the base of the transition on the thin cylinder side

P_2: is the center portion of the transition zone

P_3: at the start of the thick cylinder side, at the end of the transition zone

3.4 Results and interpretations

Computation has been carried out for different crack geometries, crack positions, different types of loading on the pipe, and the presence of a scratch on an already cracked pipe. The results for K_I are given in MPa.mm$^{0.5}$ and for an equivalent figure in MPa.m$^{0.5}$, multiply the obtained K_I value by 0.0316.

3.4.1 Effect of crack geometry

In this part, by taking five different values of the crack depth (3, 5, 7, 9 and 11) we altered the ratio a/t while maintaining the crack position at P_1. The graphs below depict the results for various crack depths under different loadings in a pipeline.

Figure 3-10 shows the behavior of the stress intensity factor "SIF" K_I along the crack front as a function of the depth of the crack (a) under traction loading.

In the present study it was found that the SIF presents the same shape of distribution for all the depths marking a maximum for the two surface points and minimums for the deepest points. This explains that the tendency of the propagation of the cracks in these cases is as much circumferential as in thickness. The maximum SIF $K_{I\,max}$ is proportional to the increase of the depth of the crack in a very tangent way for depths between a = 3 to 5 mm, beyond 5mm the slope of increase is less acute. This effect is due to the fact that the increase in the size of the crack leads to an increase in the stress field on the surface points of the crack.

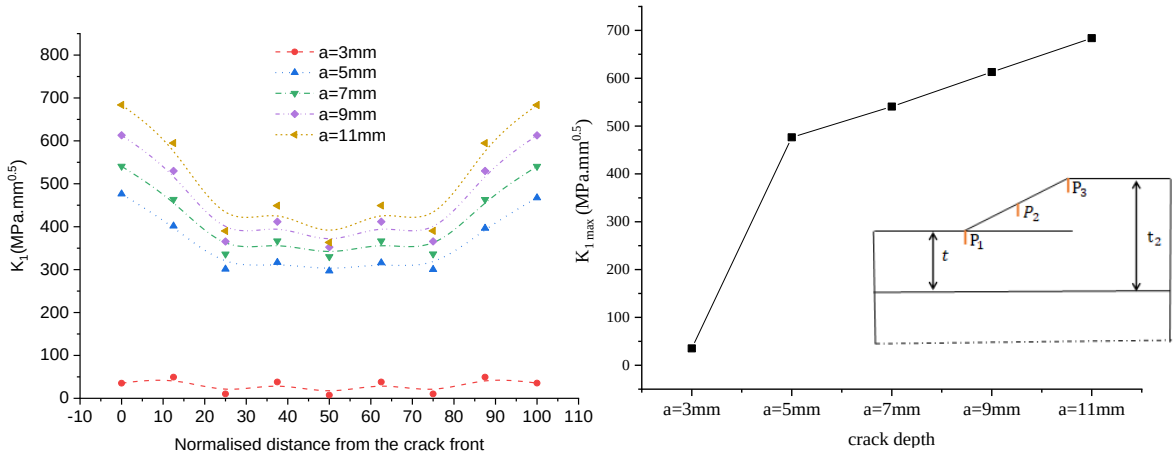

Figure 3- 10 Variation of the SIF along the crack front for different crack depths for traction loading & Variation of the $K_{I\,max}$.

It is interesting to note that the maximum values of the SIF recorded in this part are far from the critical stress intensity factor or rupture K_{IC} of API X55, the maximum value recorded is 22 MPa $m^{0.5}$ for a = 11mm while the K_{IC} at 30°C it is 162 MPa $m^{0.5}$.

Température T c°	Energie absorbée à la rupture Kv (J/cm2) (EssaiCharpy)	Résilience KCV (MJ/m2)	Ténacité JIc (MJ/m2)	Facteur d'intensité de contrainte critique KIC (MPa.√m)
30°C	123.16	1.25	3.62	162.02
20°C	120.98	1.23	2.83	160.6
10°C	107.91	1.1	2.51	151.66
0°C	99.19	1.01	2.31	145.40
-10°C	92.68	0.94	2.16	140.55
-20°C	79.57	0.81	1.85	130.23
-30°C	45.78	0.44	1.06	98.78

Table 3- 3 K_{IC} values for different temperature [53]

Figure 3-11 depicts the behavior of the stress intensity factor SIF K_I along the crack tip as a function of crack depth (a) for internal pressure loading.

The SIF distributions present negative values for most of the depths of the crack which is explained by a mesh distortion in these limit conditions and prompts us to review our CLs because the SIF values must only be positive. Also, it is clear that the values of the SIF for the depth a= 3 mm are positive and at the same time present an equivalent average with the other depths.

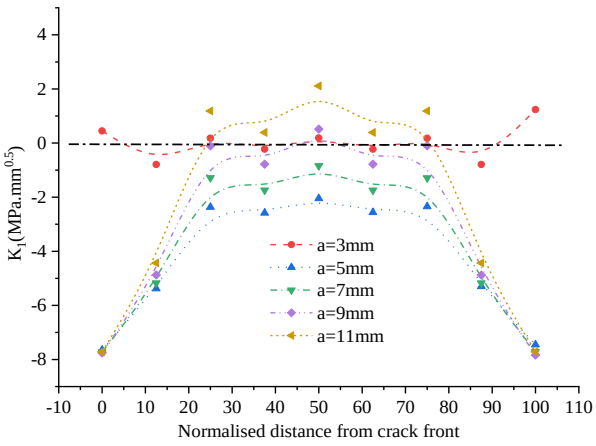

Figure 3- 11 Variation of the SIF along the crack front for different crack depths

Plotting Figure 3-12 which represents the $K_{I\,max}$ values as a function of the crack depths for an internal pressure. It can be said that the deepest points of the crack generate more stress than the surface points of the cracks for the internal pressure loading conditions.

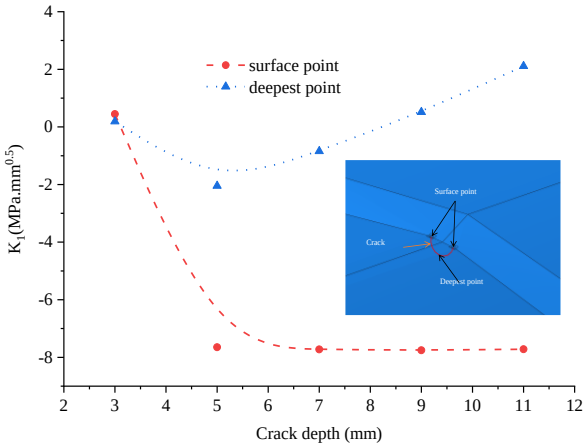

Figure 3- 12 SIF K_I as a function of crack depth at the surface and deepest point (pressure loading only).

For mixed loading (pressure – tension), Figure 3-13 shows the variation of the stress intensity factor SIF K_I along the crack front as a function of its depth (a) for a mixed loading (internal pressure + tension). This figure confirms the results of Figures 3-10. Indeed, the values of $K_{I\,max}$ are found at the surface points whereas the lowest values $K_{I\,min}$ are found at the deepest points of the semi-elliptical crack (a/c=1). The distribution of the SIF is similar to that presented in figure 3-10 except for the depth a = 3mm the values of the SIF are very low compared to others.

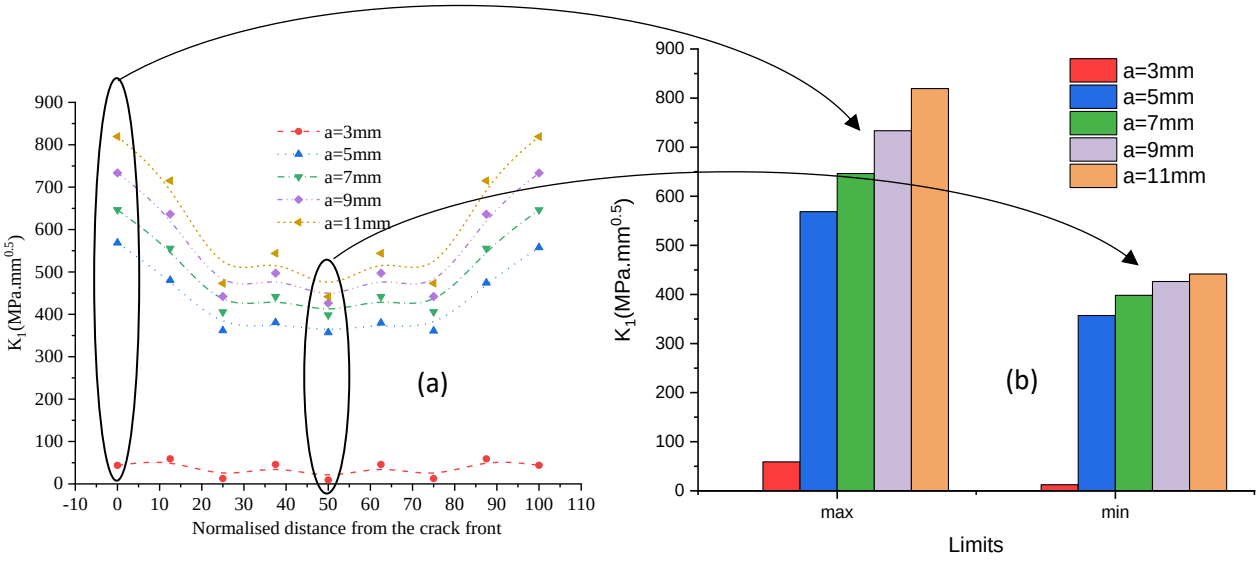

Figure 3- 13 Variation for SIF K_I for a pipe under traction - pressure loading (a) in the normalized distance along the crack front (b) Comparison of the maximum & minimum SIF for each crack depth.

To see better the effect of the variation of the depth of the crack on the values $K_{I\,min}$ and $K_{I\,max}$, one has to draw the figure 3-13 b. In this figure one can note that the two limits of the K_I are proportional to the increasing depth of the proposed crack. There is also a small difference for the depth a > 5 mm, for the depths a < 5 the SIFs are very low with a rate of 91% compared to the depth a = 5mm.

Figure 3-14 represents the $K_{I\,max}$ values as a function of the crack depths for the mixed loading. It can be seen that the surface points of the crack generate more stress than the deepest point of the cracks for the mixed loading conditions.

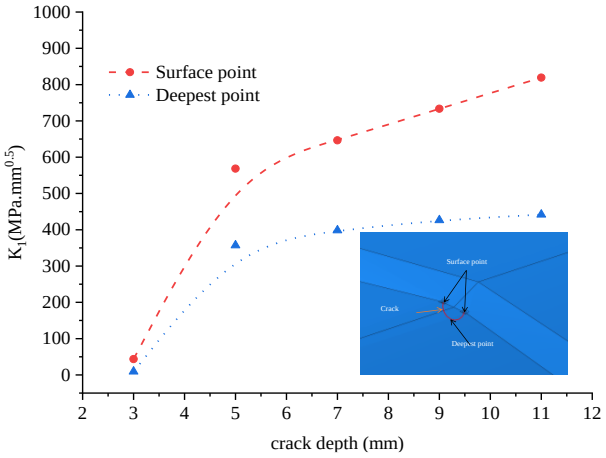

Figure 3- 14 The SIF K_I as a function of crack depth at the surface and deepest points (traction - pressure loading).

3.4.2 Effect of the type of loading and position of cracks on the pipe

Under the effect of the type of loading, the geometry of the crack was maintained (a=5mm and a/c=1) and then we varied the loading on the pipe from pressure only, tension only, and both tension and pressure at P_1. We repeated the same procedures for P_2 and P_3. The following figures illustrate the various outcomes of the setup mentioned above.

Figure 3-15 presents the variation of the stress intensity factor SIF K_I along the crack front for the position P_1 for each type of loading.

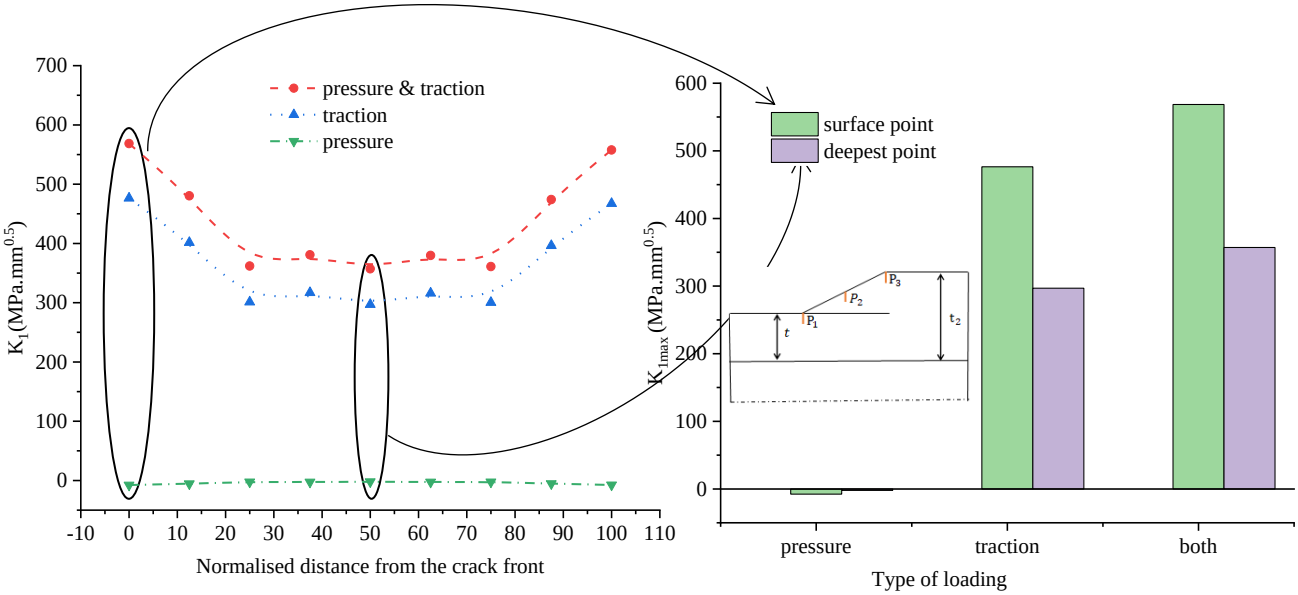

Figure 3- 15 Variation of the SIF for different pipe loadings (crack at P_1) (a) along the crack front (b) at the surface point and deepest point only.

It is noticed that there is a strong domination of the simple traction even in combination with the pressure whereas the SIF of the crack is very weak in pressure, this indicates that the opening of the lips of the crack is very favored by the traction. In another context, figure 3-15b expresses that the surface points generate stress concentrations more intense than those generated by the deepest points of the crack for the SIF max since these values in tension present a variation of 90% by compared to pressure loading only.

Finally, to confirm these results, Figure 3-16 has been plotted, which groups together the effect of the loading in relation to the position of the crack in the transition zone. It can be seen that whatever the crack position, the distribution of the SIF remains the same along the crack front for the position P_2 and P_3 with a difference in intensity, since the position of the crack P_2 records a maximum value $K_{I\,max}$ of 240 MPa $mm^{0.5}$ while that of position P_3 is almost 50% or 120 MPa.$mm^{0.5}$. This can be explained by the effect of the non-linearity of the geometry of the transition zone which leads to a non-uniform distribution of the stresses.

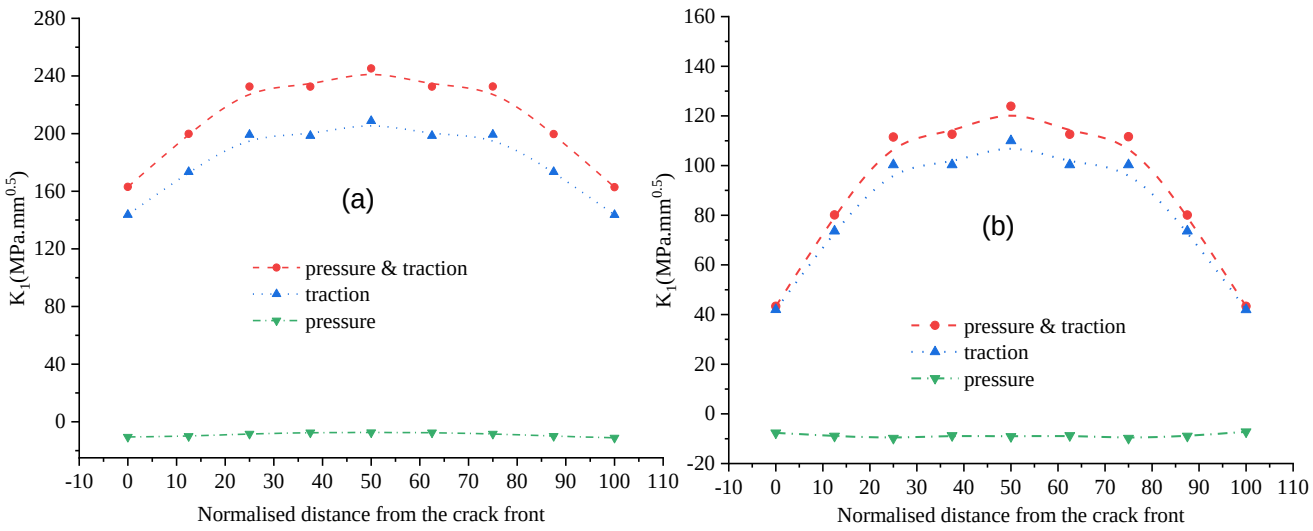

Figure 3- 16 Variation of the SIF along the crack front for different pipe loadings (a) crack at P_2, (b) crack at P_3

It should also be noted that for the position P_1 the SIF $K_{I\,max}$ is marked on the surface points of the crack whereas for the crack in position P_2 and P_3 it is found on the deepest point.

To effectively comprehend the effect of the crack's position, we compared the behavior of a crack (a=5mm and a/c=1) in a pipe with thickness transition at P_1, P_2 and P_3 to that of the same crack in a pipe without thickness transition at P_4. Considering that the pipes were under both traction and pressure loading.

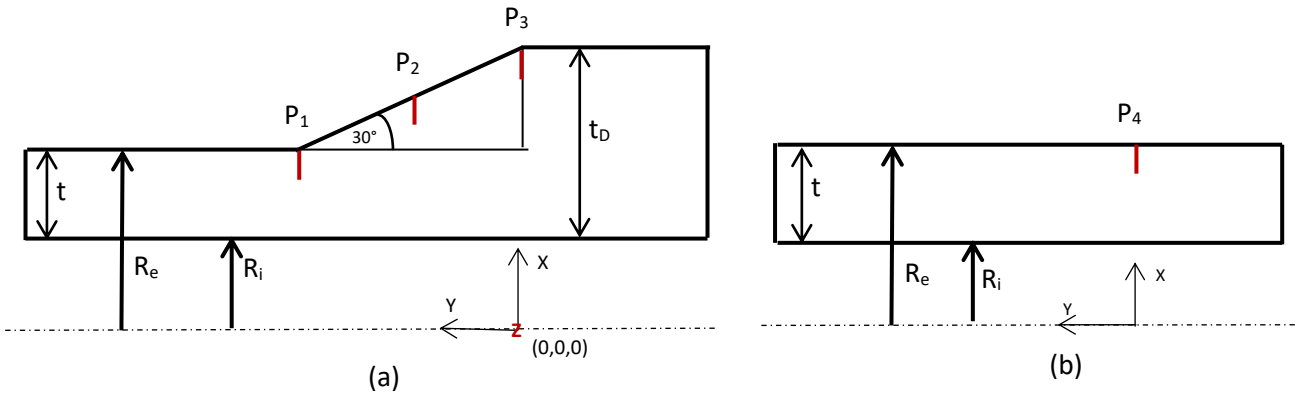

Figure 3- 17 Positions of the crack (a) in a pipe with thickness transition (b) in a pipe without thickness transition.

Figure 3-18 shows the variation of the stress intensity factor SIF K_I along the crack front for different positions of crack under mixed loading. It is noticed that the P_1 position of the crack marks the highest value and an inverse distribution of the SIF compared to the other positions on the pipeline. The pipeline with uniform thickness without transition zone presents less danger of crack propagation since it has very low values than that in the transition zone. The representation of SIFs in figure (b) shows clearly that the use of transition zones in the transport of hydrocarbons should be avoided as much as possible because it can easily be a crack propagation initiation zone.

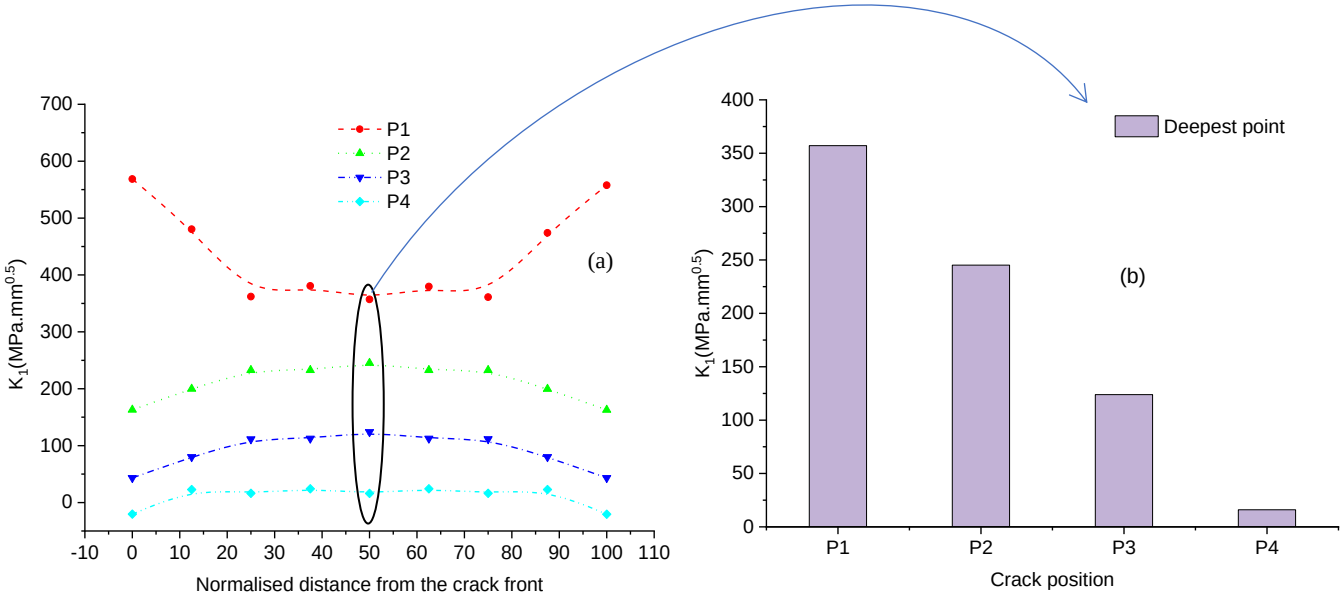

Figure 3- 18 Variation of the SIF in different crack positions (a) along the normalized distance from the crack front (b) at the deepest point only

3.4.4 Effect of the interaction of a scratch on a cracked pipe

A scratch was introduced to a pipe under both pressure and traction loading with a crack at the base of the transition zone (P_1). To thoroughly investigate the influence of this scratch, we changed its position from along the transition zone to the thinner part of our pipe (S_1 to S_5). The geometry of the scratch and the various positions where it was placed are shown in the figure below.

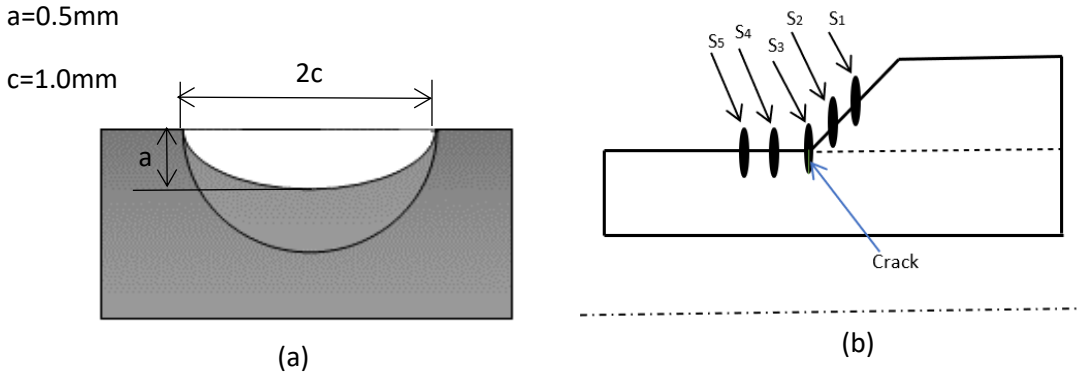

Figure 3- 19 Scratch model's (a) geometry (b) various positions

The variation of the stress intensity factor SIF KI along the crack front for the position of the scratch is plotted in Fig. 3-20 (a), it can be said that the distribution of the SIF is independent of the presence of the scratch but the surface points of the crack are sensitive to its presence, which is visible in Fig. 3-20(b).

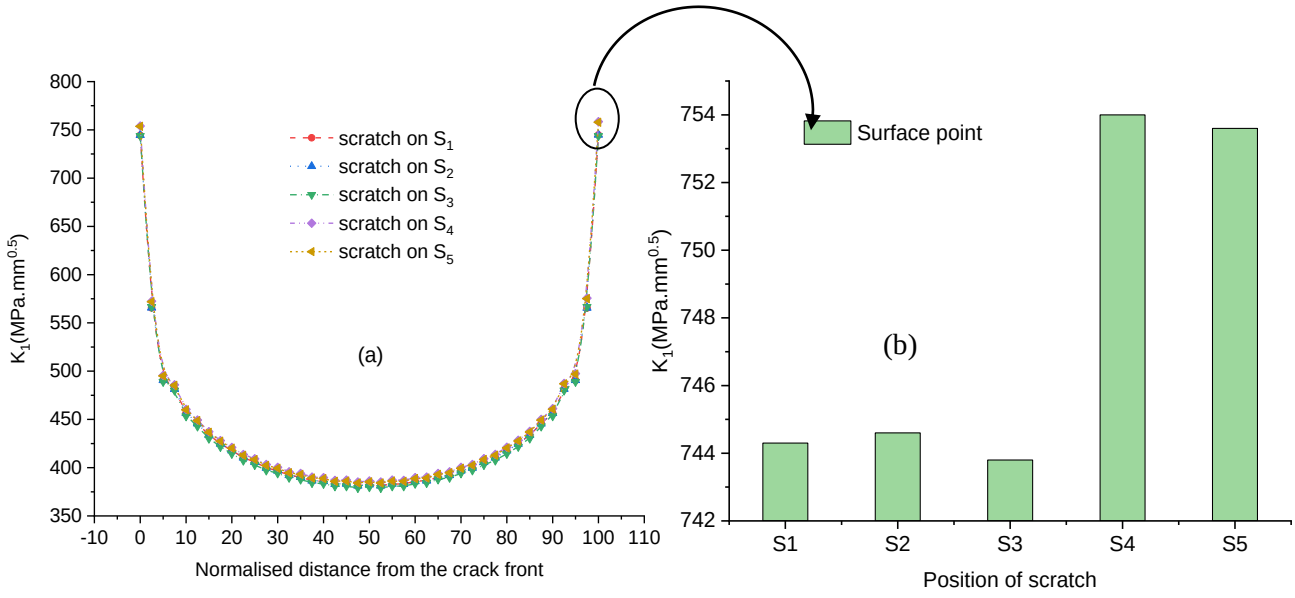

Figure 3- 20 Variation of the SIF K_I for a pipe under traction - pressure loading (a) in the normalized distance along the crack front (b) at the surface point only (traction-pressure loading.

Indeed, the values of the SIF Max are practically stable for the positions S_1, S_2 and S_3 however the positions S_4 and S_5 mark a small increase of 2%.

We think we had to increase the size of the scratch to have a visible effect, but it was not possible because we encountered mesh problems each time.

3.4.5 General comparison of a cracked pipe with a uniform thickness, with thickness transition and with a scratch

Subsequently, we compared the variation of the SIF in three different conditions of a pipe: a pipe with uniform thickness, a pipe with a thickness transition, and a scratched pipe with a thickness transition. The size of the crack is constant (a=5mm and a/c=1) in all the pipes under comparison and all the pipes are under both pressure and traction loading.

In this last part we expressed the variation of the stress intensity factor SIF K_I along the crack front for different configurations in Figure 3-21 (a). Where it is clear that the presence of the scratch with a crack in a transition zone increases strongly the maximum SIF values on the surface points of the crack compared to a pipeline with a crack only, Figure 3-21 (b) shows clearly the gap recorded by the combination of a crack in a transition zone with a scratch which is considered harmful to the integrity of the pipeline.

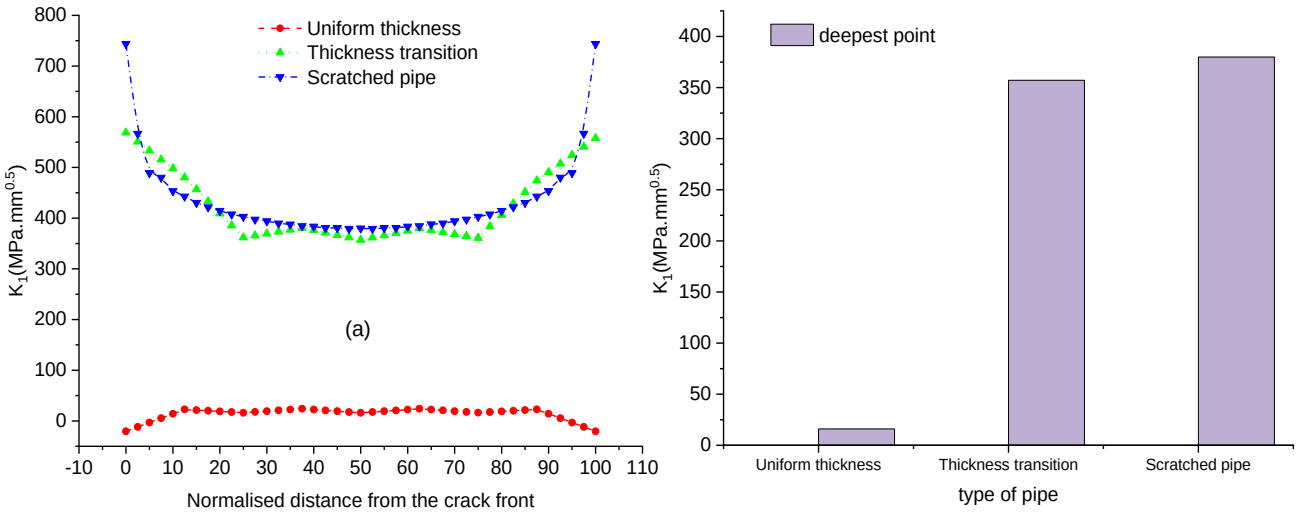

Figure 3- 21 Variation of the SIF in different crack positions on different pipes under traction and pressure loading (a) along the normalized distance from the crack front (b) at the deepest point only.

CONCLUSION

The results obtained numerically by the three-dimensional finite element method allow the following conclusions to be drawn:

- For all the depths marking a maximum at the two surface points and minimums at the deepest points, this explains that the tendency of the propagations of the cracks in these cases is as much circumferential as in thickness.

- That the maximum values of the SIF recorded in this part are far from the critical stress intensity factor or rupture K_{IC} of API X55, the maximum value recorded is 22 MPa $m^{0.5}$ for a = 11 mm while the K_{IC} at 30°C it is 162 MPa $m^{0.5}$.

- The values of $K_{I\text{-}max}$ are found on the points of surfaces whereas the lowest values $K_{I\text{-}min}$ are found on the deepest points of the semi-elliptical crack (a/c=1).

- That the two limits of the K_I are proportional to the increasing depth of the proposed crack. There is also a small difference for the depth a > 5 mm, for the depths a < 5 the SIFs are very low with a rate of 91% compared to the depth a = 5mm.

- It is noticed that there is a strong domination of the simple traction even in combination with the pressure whereas the SIF of the crack is very weak in pressure this indicates that the opening of the lips of the crack is very favored by the traction.

- In another context in figure 3-15b expresses that the surface points generate stress concentrations more intense than those generated by the deepest points of the crack for the SIF max since these values in tension present a variation of 90% compared to pressure loading only.

- the presence of the scratch with a crack in a transition zone increases strongly the maximum SIF values on the surface points of the crack compared to a pipeline with a crack only.

- The SIF is independent of the presence of the scratch but the surface points of the crack are sensitive to its presence, which is visible in Fig. 3-20(b). Indeed, the values of the SIF $_{Max}$ are practically stable for the positions S_1, S_2 and S_3 however the positions S_4 and S_5 mark a small increase of 2%.

– The pipeline with uniform thickness without transition zone presents less danger of crack propagation compared to pipeline with a thickness transition.

BIBLIOGRAPY

[1] F. Campbell, Fatigue and fracture: understanding the basics, Materials Park,Ohio: ASL International, 2012.

[2] G. R. Iwrin, "Analysis of Stresses and Strains Near the End of a Crack Traversing a Plate," *Journal of Applied Mechanics,* vol. 24, no. 3, pp. 361-364, 1957.

[3] P. Kumar, Element of Fracture Mechanics, New Delhi: Tata McGraw-Hill Publishing Company Limited, A009.

[4] V. Kumar, . M. German and . C. Shih, "Engineering approach for elastic-plastic fracture analysis," General Electric Co., Schenectady, NY (USA). Corporate Research and Development Dept, USA, 1981.

[5] N. Bhavsar, K. Brahmbhatt and . D. Patel, "Researchgate," 25 March 2020. [Online]. Available: https://www.researchgate.net/publication/340135214. [Accessed 10 June 2023].

[6] J. . L. Swedlow, "On Griffith's theory of fracture," *International Journal of Fracture Mechanics,* vol. 1, no. 3, p. 210–216, 1965.

[7] B. C. Patel, B. Gupta and A. Choubey, "Experimental And Numerical Analysis Of Critical Stress Intensity Factor Of Pressure Vessel Material Used In Disc Shaped Compact Specimen," *International Journal of Engineering Research,* vol. 8, no. 1, 2012.

[8] M. Janssen, J. Zuidema and R. Wanhill, Fracture Mechanics, 2nd Edition, Delft: VSSD, 2006.

[9] S. Thorat, "Learnmech.com," [Online]. Available: https://learnmech.com/introduction-brittle-failure-brittle-failure-occurs/#Introduction_To_Brittle_Failure-_How_Brittle_Failure_Occurs. [Accessed 11 April 2023].

[10] W. a. M. Garrison, "Ductile fracture," 18 February 1987. [Online]. Available: https://www.researchgate.net/publication/222256132. [Accessed 10 March 2023].

[11] J. M. Barsom, Fracture and fatigue control in structures: applications of fracture mechanics, 2nd Edition, Eaglewood Cliffs N.J:: Prentice-Hall, 1987.

[12] T. L. Anderson, Fracture Mechanics: Fundamentals and Applications, 2nd Edition, Texas: CRC Press LLC, 1994.

[13] C. H. Wang, "Introduction to Fracture Mechanics," DSTO Aeronautical and Maritime Research Laboratory, Melbourne Victoria 3001, 1996.

[14] R. W. Hertzberg, R. P. Vinci and J. L. Hertzberg, Deformation and Fracture Mechanics of Engineering Materials, 5th Edition, Hoboken: John Wiley & Sons, Inc., 2008.

[15] A. A. Griffith, "VI. The phenomena of rupture and flow in solids," *Philosophical Transactions of the Royal Society of London. Series A, Containing Papers of a Mathematical or Physical Character,* vol. 221, pp. 163-198, 1921.

[16] E. Orowan, "Fracture and Strength of Solids, Reports on Progress in Physics," *Open Journal of Metal,* vol. 8, pp. 185-232, 1948.

[17] J. R. Rice, "Elastic-plastic fracture mechanics,," *Engineering Fracture Mechanics,* vol. 5, no. 4, pp. 1019-1022, 1973.

[18] W. Khor, Moore,P., Pisarski,H. and Brown,C., ""Comparison of methods to determine CTOD for SENB specimens in different strain hardening steels," *Fatigue & Fracture of Engineering Materials & Structures,* vol. 41, no. 3, pp. 551-564, 2018.

[19] M. Abderrahim, «Ingénierie des systèmes mécaniques productiques,» UNIVERSITE ABOU BEKR BELKAID-TLEMCEN, TLEMCEN, Année universitaire 2012-2013.

[20] J. Schijve , Fatigue of structures and materials, Dordrecht: Springer, 2010.

[21] E. J. Hean, "Mechanics of Materials: an introduction to the mechanics of elastic and plastic deformation of solids and structural materials, 3rd Edition," Butterworth-Heinemann, Oxford; Boston, 1997.

[22] L. Henry, "Britannica," 26 May 2023. [Online]. Available: https://www.britannica.com/technology/pipeline-technology. [Accessed 30 March 2023].

[23] E. Repko, "U.S. Government Accountablity Office," 26 January 2022. [Online]. Available: https://www.gao.gov/products/gao-22-105140. [Accessed 6 March 2023].

[24] M. Saleh, "Pipeline Construction (Classification, welding, construction, inspection)," University of Alexandria, 2017.

[25] G. A. Antaki, Piping and Pipeline Engineering, Aiken, South Carolina, U.S.A: MARCEL DEKKER, INC, 2005.

[26] N. S. Nandagopal, Pipeline Systems: Design, Construction, Maintenance and Asset Management, Revised Edition, United States of America: DC Technologies, 2007.

[27] "The Constructor," [Online]. Available: https://theconstructor.org/structural-engg/structural-design/types-pipeline-construction-method/1854/. [Accessed 19 Feburary 2023].

[28] "TWI," The welding institute, [Online]. Available: https://www.twi-global.com/technical-knowledge/faqs/what-is-pipe-welding#TypesOfWeldingUsed. [Accessed 12 May 2023].

[29] "ZipRecruiter," [Online]. Available: https://www.ziprecruiter.com/career/Pipeline-Welder/What-Is-How-to-Become. [Accessed 3 May 2023].

[30] K. Nagarajan, "Design of Structures," 5 October 2013. [Online]. Available: http://ecoursesonline.iasri.res.in/mod/page/view.php?id=127486. [Accessed 25 April 2023].

[31] D. Bingham, "Los Alamos National Laboratory," Triad National Security, LLC, [Online]. Available: https://engstandards.lanl.gov/ESM_Ch13.shtml. [Accessed 10 June 2023].

[32] T. C. Pharris and R. L. Kolpa, Overview of the Design, Construction, and Operation of Interstate Liquid Petroleum Pipelines, Oak Ridge: Argonne National Laboratory, 2007.

[33] "Corrosionpedia," 11 January 2019. [Online]. [Accessed April 26 2023].

[34] E. S. Van, H. J. Sjors, A. . M. Gresnigt, D. Vasilikis and S. A. Karamanos, "Ultimate bending capacity of spiral-welded steel tubes – Part I: Experiments," *Thin-Walled Structures,* vol. 102, pp. 286-304, 2016.

[35] "The Process Piping," [Online]. Available: https://www.theprocesspiping.com/introduction-to-welded-pipe-manufacturing/. [Accessed 28 April 2023].

[36] "Total Materia," January 2019. [Online]. Available: https://www.totalmateria.com/page.aspx?ID=CheckArticle&site=kts&NM=544. [Accessed 14 April 2023].

[37] K. Kusakana, 31 May 2021. [Online]. Available: https://www.researchgate.net/publication/351998208. [Accessed 1 June 2023].

[38] "Trenchlesspedia," 9 December 2017. [Online]. Available: Available: https://www.trenchlesspedia.com/definition/2477/cracks. [Accessed 15 March 2023].

[39] "Rosen," Rosen empowered by technology, [Online]. Available: https://www.rosen-group.com/global/solutions/services/pipeline-cracks. [Accessed 15 June 2023].

[40] "GeoCorr Blog," 20 May 2021. [Online]. Available: https://www.gao.gov/assets/gao-22-105140.pdf. [Accessed 5 April 2023].

[41] M. Baler, "Understanding Stress Corrosion Cracking (SCC) in pipelines," *OPS TT08 Final Draft-Stress Corrosion Cracking Study,* pp. 15-28, 2004.

[42] S. M. G. a. R. Sarrafan, "Weld Metal Hydrogen Cracking in Transmission Pipelines Construction," in *in 2010 8th International Pipeline Conference*, Calgary, Alberta, Canada, 2010.

[43] "NPC VTD," [Online]. Available: https://www.npcvtd.ru/en/services/vnutritrubnaya-diagnostika/. [Accessed 3 April 2023].

[44] M. J. Baker, "Mechanical Damage FINAL REPORT," U.S. Department of Transportation Pipeline and Hazardous Materials Safety Administration Office of Pipeline Safety, Washington, D.C, éààç.

[45] "Nigen," 6 August 2020. [Online]. Available: https://nigen.com/pipeline-integrity-management-planning-management-services/. [Accessed 26 May 2023].

[46] "amarineblog," [Online]. Available: https://amarineblog.com/2020/10/04/what-is-caliper-pig-pipeline-inspection/. [Accessed 9 March 2023].

[47] "Jettyrobot," [Online]. Available: https://www.jettyrobot.com/industry/inspection-of-pipelines. [Accessed 19 May 2023].

[48] "wermac," [Online]. Available: https://www.wermac.org/documents/unequal_wallthickness.html. [Accessed 20 May 2023].

[49] "TC Energy," 2020-2021. [Online]. Available: https://www.tcenergy.com/sustainability/safety/pipeline-and-operations/. [Accessed 7 May 2023].

[50] B. SIMULIA, Abaqus 6.11: Abacus/CAE user's Manual, Analysis Dassault Systèmes, 2013.

[51] MEDJDOUB Meriem and ERROUANE Houria, "Comportement en rupture d'une fissure circonférentielle dans un pipeline soumis au chargement mixte (Pression, moment et traction)," 2019/2020.

[52] API 5L. Specification for line pipe. API specification 5L, 42nd Edition, USA: The American Petroleum Institute, 2000.

[53] A. IKHLEF, 2015/2016. [Online]. Available: https://biblio.univ-annaba.dz/ingeniorat/wp-content/uploads/2018/10/Ikhlef-Abdelmalek.pdf. [Accessed 2 June 2023].